

# Convex Recovery of Marked Spatio-Temporal Point Processes

Anatoli Juditsky, Arkadi Nemirovski, Liyan Xie, Yao Xie

February 28, 2022

## Contents

<b>1</b>	<b>Introduction</b>	<b>2</b>
<b>2</b>	<b>Recovery for spatio-temporal Bernoulli process</b>	<b>3</b>
2.1	Single-state model . . . . .	4
2.2	Least Squares estimate . . . . .	5
2.3	Performance guarantees . . . . .	7
2.3.1	Upper-bounding risk . . . . .	8
2.3.2	Confidence intervals for linear forms of $\beta$ . . . . .	9
2.4	Extensions: Recovery for multi-state spatio-temporal processes . . . . .	10
<b>3</b>	<b>Nonlinear link function</b>	<b>12</b>
3.1	Single-state process . . . . .	12
3.2	Multi-state processes . . . . .	14
<b>4</b>	<b>Maximum Likelihood estimate</b>	<b>15</b>
4.1	ML estimate for single and multi-state . . . . .	15
4.2	Performance guarantee . . . . .	15
4.3	ML estimate with general link function . . . . .	17
<b>5</b>	<b>Simulation study</b>	<b>18</b>
5.1	Single state spatio-temporal processes . . . . .	18
5.2	Multi-state spatio-temporal processes . . . . .	19
5.3	Sparse recovery . . . . .	21
<b>6</b>	<b>Real data study</b>	<b>22</b>
6.1	Crime events in Atlanta . . . . .	22
6.2	Novel coronavirus spread in China . . . . .	24
<b>7</b>	<b>Conclusion</b>	<b>27</b>

## Abstract

We present a multi-dimensional Bernoulli process model for spatial-temporal discrete event data with categorical marks, where the probability of an event of a specific category in a location may be influenced by past events at this and other locations. The focus is to introduce general forms of influence function, which can capture an arbitrary shape of influence from historical events, between locations, and between different categories of events. The general form of influence function differs from the commonly adapted exponential delaying function over time, and more importantly, in our model, we can learn the delayed influence of prior events, which is an aspect seemingly largely ignored in prior literature. Prior knowledge or assumptions on the influence function are incorporated into our framework by allowing general convex constraints on the parameters specifying the influence function. We develop two approaches for recovering these parameters, using the constrained least-square (LS) and maximum likelihood (ML) estimations. We demonstrate the performance of our approach on synthetic examples and illustrate its promise using real data (crime data and novel coronavirus data), in extracting knowledge about the general influences and making predictions.

*Dedicated to people fighting with novel coronavirus.*

## 1 Introduction

Discrete events are a type of sequential data, where each data point is a tuple consisting of event time, location, and category. Such event data is ubiquitous in modern applications, including police reports [10], electronic health records, traffic incidents, social networks [8], and so on. In modeling discrete events, we are particularly interested in estimating the triggering (or inhibiting) effect of the events (see [15] for an overview). For example, in crime analysis, the triggering effect has been empirically verified, when an event happens, it makes the future events more likely to happen in the neighborhood. Similar empirical observation has been made for other applications.

Recently, the so-called Hawkes processes [6, 5, 7] have become popular in modeling the triggering effect, possibly over time, space, or networks (where events at one node will trigger events at neighboring nodes). The Hawkes process is a type of mutually-exciting non-homogeneous point process, where the intensity has a stochastic part that depends on the past event. Along this line of the model, there are other types of point process modeling, where different “link” functions are considered, such as self-correcting process, reactive process, and Bernoulli process [9]. These point processes model the interactions between events using an *influence function*. So-far, much research effort in this domain has been focusing on temporal process modeling. The study of more complex modeling the spatial aspects, especially jointly with discrete marks, is still in infancy.

In this paper, we present a general computational framework for estimating the marked spatio-temporal processes with (categorical) marks. We consider the Bernoulli process, first in the single-state setting where observations are either binary (to indicate whether or not an event has happened), as a natural simplification of the continuous-time Hawkes process, in the discrete-time and discrete space setting. Then we generalize to the multi-state setting to incorporate categorical marks. Similar to other self- and mutual point processes models, we model dependence and triggering effect through linear linkage and general linkage functions. A notable feature of our model is that we allow the influence function to be completely general, for example (1) the influence does not have to be monotonically decaying, which is a common assumption used in existing work; (2) the influence function can have delays, which is an aspect largely ignored in existing work since most work assumes that the influence kernel function is a monotonic decaying function that starts immediately from the event time. This

generality comes from the fact that in our model, prior information on the structure of the influence should be presented by (whatever) convex constraints on the parameters, which is quite flexible. We cast the influence function recovery problem using two approaches: (1) the least-square (LS) estimate, and (2) the maximum likelihood (ML) estimate. We take a variational inequality formulation to address the resulted optimization problem, which enables us to obtain interpretable performance bounds and confidence intervals for the estimates, and computationally efficient algorithms. We demonstrate the good performance of our LS and ML estimators on simulated experiments and using real-world data, in estimating the influence functions on crime data and the spread of recent novel coronavirus.

In summary, several features of our approach: (i) Our parametric assumption on the influence function is completely general. This is drastically different from the classical approach, which assumes the time influence decays exponentially in time. (ii) We directly model the interactions of historical events with future events, at different locations, across different categories. (iii) With our approach, the estimate is specified as a solution to an efficiently solvable problem with a convex structure, *variational inequality with monotone operator*; while the maximum likelihood estimation with concave log-likelihood is in the scope of this approach, this scope is in no sense restricted to this special case. Then we generalize our approach to multiple category observation and general link functions.

**Related Work.** The model we consider here is related to information diffusion process over continuous time, for example, Hawkes model over networks (see [15] for an overview), and information diffusion networks with survival analysis [4]. Compared with these well-known models in continuous time, with our approach, we discretize space and time, which leads to the spatio-temporal Bernoulli process. This is a simplification that, nonetheless, will lead to practical algorithms that can be used in real scenarios. Recent work [1] considers general link function (rather than commonly assumed linear link function) for Hawkes process.

A related line of work is the non-parametric Hawkes process estimation [3, 17, 11] based on the Expectation-Maximization (EM) algorithms and Kernel method. This paper proposes a different approach based on convex optimization and sheds insights on the performance guarantees for the recovery routines.

There is also much work considering the estimation of information diffusion networks under the Bayesian framework. For example, [9] considers the number of events in discrete time intervals with equal duration. [2] considers a continuous-time model and estimate the parameters using both maximum likelihood estimator and Bayesian methods. [14] considers a Bernoulli model similar to ours, but they estimate parameters using the Bayesian approach and impose prior distributions on parameters. [13] also considers a Bayesian framework with applications in retail market analytics. In contrast, what follows is *not* in the Bayesian framework.

## 2 Recovery for spatio-temporal Bernoulli process

Consider spatio-temporal Bernoulli process with discrete space and time. Specifically, we assume that the spatio-temporal grid we deal with is fine enough so that we can neglect the possibility for more than one event to occur in a cell of the grid. We will model the interactions of these events in the grid.

## 2.1 Single-state model

We define a *spatio-temporal Bernoulli process with memory depth  $d$*  as follows. We observe on discrete time horizon  $\{t : -d + 1 \leq t \leq N\}$  random process as follows. At time  $t$  we observe Boolean vector  $\omega_t \in \mathbf{R}^K$  with entries  $\omega_{tk} \in \{0, 1\}$ ,  $1 \leq k \leq K$ . Here  $\omega_{tk} = 1$  and  $\omega_{tk} = 0$  mean, respectively, that at time  $t$  in location  $k$  an event took/did not take place. We set

$$\begin{aligned}\omega^t &= \{\omega_{sk}, -d + 1 \leq s \leq t, 1 \leq k \leq K\} \in \mathbf{R}^{(t+d) \times K}, \\ \omega_\tau^t &= \{\omega_{sk}, \tau \leq s \leq t, 1 \leq k \leq K\} \in \mathbf{R}^{(t-\tau+1) \times K}.\end{aligned}$$

In other words,  $\omega^t$  denotes all observations (at all locations) until current time  $t$ , and  $\omega_\tau^t$  contains observations on time horizon from  $\tau$  to  $t$ .

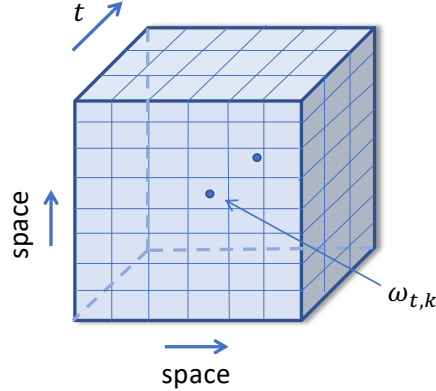


Figure 1: Illustration of the discretized process.

We assume that for  $t \geq 1$  the conditional probability of the event  $\omega_{tk} = 1$ , given the history  $\omega^{t-1}$ , is specified as

$$\beta_k + \sum_{s=1}^d \sum_{\ell=1}^K \beta_{k\ell}^s \omega_{(t-s)\ell}, \quad 1 \leq k \leq K, \quad (1)$$

where  $\beta = \{\beta_k, \beta_{k\ell}^s : 1 \leq s \leq d, 1 \leq k, \ell \leq K\}$  is a collection of coefficients. Here

- $\beta_k$  corresponds to the *baseline intensity* at the  $k$ -th location (i.e., the intrinsic probability for an event to happen at a location without the endogenous influence, also called the birthrates);
- $\beta_{k\ell}^s$  captures the magnitude of the *influence* of an event that occurs at time  $t - s$  at the  $\ell$ -th location on chances for an event to happen at time  $t$  in the  $k$ -th location; so the sum term represents the cumulative influence at the  $k$ -th location from the events in the past.

Since the probability of occurrence is between 0 and 1, we require the coefficients to satisfy

$$\begin{aligned}0 &\leq \beta_k + \sum_{s=1}^d \sum_{\ell=1}^K \min[\beta_{k\ell}^s, 0], \quad \forall k \leq K, \\ 1 &\geq \beta_k + \sum_{s=1}^d \sum_{\ell=1}^K \max[\beta_{k\ell}^s, 0], \quad \forall k \leq K.\end{aligned} \quad (2)$$

Figure 2 illustrates a realization of the sample path of a simple Bernoulli process under our setting with different memory depths (5 for the top figure and 0 for the bottom). Note that in the bottom plot, the events are more spread out because of the choice of the coefficients and since the memory depth is 0 (no influence over time).

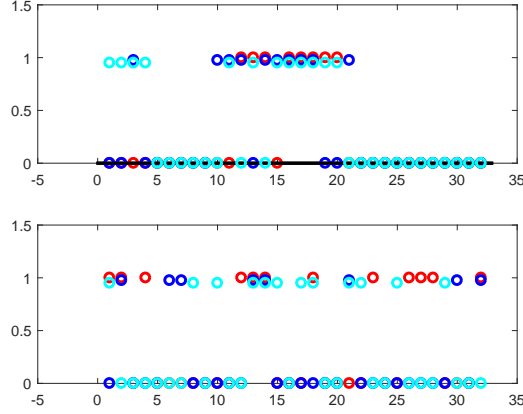


Figure 2: Realizations of one-dimensional spatio-temporal Bernoulli processes with memory depths 5 (top) and 0 (bottom) with three spatial locations on time horizon  $N = 32$ . Events in different locations are marked by different colors. The  $y$ -axis “0” means no event, and “1” means event. The total number of events in the realization is 30 (top) and 32 (bottom).

Our goal is to recover the collection of parameters  $\beta$  using a set of observations  $\omega^N$  over a time horizon  $N$ . In this paper, we consider two approaches for solving the recovery problem based on least-square and maximum likelihood. We will show both approaches can be cast as convex optimization problems.

## 2.2 Least Squares estimate

Define the cardinality number

$$\kappa = K + dK^2.$$

Let us arrange all reals from the collection  $\beta$  in (1) into a column vector (still denoted  $\beta$ ):

$$\beta = [\beta_1, \dots, \beta_K, \beta_{11}^1, \dots, \beta_{11}^d, \beta_{1K}^1, \dots, \beta_{1K}^d, \dots, \beta_{KK}^1, \dots, \beta_{KK}^d]^T \in \mathbb{R}^\kappa.$$

Note that constraint (2) above states that  $\beta$  must reside in the polyhedral set  $\mathcal{B}$  given by explicit polyhedral representation<sup>1</sup>. Assume that we are given a convex compact set  $\mathcal{X} \subset \mathcal{B}$  such that  $\beta \in \mathcal{X}$ . Our model says that for  $t \geq 1$ , the conditional expectation of  $\omega_t$  given  $\omega^{t-1}$  is  $\eta^T(\omega_{t-d}^{t-1})\beta$ , for a known to us function  $\eta(\cdot)$ , which is defined on the set of all zero-one arrays  $\omega_{t-d}^{t-1} \in \{0, 1\}^{d \times K}$  and taking values in the matrix space  $\mathbf{R}^{\kappa \times K}$

$$\eta^T(\omega_{t-d}^{t-1}) = [I_K, I_K \otimes \text{vec}(\omega_{t-d}^{t-1})^T] \in \mathbf{R}^{K \times \kappa}, \quad (3)$$

<sup>1</sup>Polyhedral representation of a set  $X \subset \mathbf{R}^n$  is representation of the form

$$X = \{x \in \mathbf{R}^n : \exists w \in \mathbf{R}^m : Px + Qw \leq r\},$$

that is, representation of  $X$  as a projection of the solution set of a system of linear inequalities in the space of  $(x, w)$ -variables on the plane of  $x$ -variables. When  $X$  is polyhedrally representable, it automatically is polyhedral – can be represented by finite system of linear inequalities in  $x$ -variables only. This system, however, can be much larger than the one in the polyhedral representation in question, making explicit polyhedral representations the standard descriptions of polyhedral sets in optimization.

where  $I_K$  is the identity matrix,  $\otimes$  denotes the standard Kronecker product, and  $\text{vec}(\cdot)$  vectorizes a matrix by stacking all column. Note that the matrix  $\eta(\omega_{t-d}^{t-1})$  is Boolean and has at most one nonzero entry in every row<sup>2</sup>.

Consider the vector field  $F(x) : \mathcal{X} \rightarrow \mathbf{R}^\kappa$ , defined as

$$F(x) = \frac{1}{N} \mathbf{E}_{\omega^N} \left\{ \sum_{t=1}^N [\eta(\omega_{t-d}^{t-1}) \eta^T(\omega_{t-d}^{t-1}) x - \eta(\omega_{t-d}^{t-1}) \omega_t] \right\} : \mathcal{X} \rightarrow \mathbf{R}^\kappa$$

where  $\mathbf{E}_{\omega^N}$  denotes expectation taken with respect to  $\omega^N$  (and other  $\mathbf{E}_{\omega^t}$  are similarly defined). Below, all expectations and probabilities are conditional and the condition is the specific realization of the initial part  $\omega_{-d+1}^0$  of observations.

Observe that we have

$$\langle F(x) - F(y), x - y \rangle = \frac{1}{N} \sum_{t=1}^N \mathbf{E}_{\omega^N} \{ (x - y)^T \eta(\omega_{t-d}^{t-1}) \eta^T(\omega_{t-d}^{t-1}) (x - y) \} \geq 0, \quad \forall x, y \in \mathcal{X}.$$

Thus, this vector field  $F$  is *monotone*.<sup>3</sup> Moreover, we have  $F(\beta) = 0$ , since

$$\begin{aligned} F(\beta) &= \frac{1}{N} \mathbf{E}_{\omega^N} \left\{ \sum_{t=1}^N [\eta(\omega_{t-d}^{t-1}) \eta^T(\omega_{t-d}^{t-1}) \beta - \eta(\omega_{t-d}^{t-1}) \omega_t] \right\} \\ &= \frac{1}{N} \sum_{t=1}^N \mathbf{E}_{\omega^t} \{ \eta(\omega_{t-d}^{t-1}) \eta^T(\omega_{t-d}^{t-1}) \beta - \eta(\omega_{t-d}^{t-1}) \omega_t \} \\ &= \frac{1}{N} \sum_{t=1}^N \mathbf{E}_{\omega^{t-1}} \{ \eta(\omega_{t-d}^{t-1}) \eta^T(\omega_{t-d}^{t-1}) \beta - \mathbf{E}_{\omega_t | \omega^{t-1}} [\eta(\omega_{t-d}^{t-1}) \omega_t] \} \\ &= \frac{1}{N} \sum_{t=1}^N \mathbf{E}_{\omega^{t-1}} \{ \eta(\omega_{t-d}^{t-1}) \eta^T(\omega_{t-d}^{t-1}) \beta - \eta(\omega_{t-d}^{t-1}) \eta^T(\omega_{t-d}^{t-1}) \beta \} = 0, \end{aligned}$$

where  $\mathbf{E}_{\omega_t | \omega^{t-1}}$  denotes the expectation taken with respect to the conditional distribution of  $\omega_t$  conditioned on  $\omega^{t-1}$ . Therefore,  $\beta \in \mathcal{X}$  is a zero of  $F$  and therefore is a solution to the variational inequality:

$$\text{find } z \in \mathcal{X} : \langle F(w), w - z \rangle \geq 0, \quad \forall w \in \mathcal{X}, \quad \text{VI}[F, \mathcal{X}]$$

with monotone operator  $F$ .

Now consider the empirical version of the vector field. With  $A[\omega^N]$  and  $a[\omega^N]$  defined accordingly below, we note that our full observation  $\omega^N$  provides us with monotone and affine *empirical vector field*

$$F_{\omega^N}(x) = \underbrace{\left[ \frac{1}{N} \sum_{t=1}^N \eta(\omega_{t-d}^{t-1}) \eta^T(\omega_{t-d}^{t-1}) \right]}_{A[\omega^N]} x - \underbrace{\frac{1}{N} \sum_{t=1}^N \eta(\omega_{t-d}^{t-1}) \omega_t}_{a[\omega^N]}, \quad (4)$$

such that the expected value of this field, at every point  $x$ , is  $F(x)$ . We propose to use, as an estimate of  $\beta$ , a weak solution to the Sample Average Approximation of  $\text{VI}[F, \mathcal{X}]$ , i.e., the variational inequality

$$\text{find } z \in \mathcal{X} : \langle F_{\omega^N}(w), w - z \rangle \geq 0, \quad \forall w \in \mathcal{X}. \quad \text{VI}[F_{\omega^N}, \mathcal{X}]$$

The monotone vector field  $F_{\omega^N}(\cdot)$  is continuous (even affine), so that the weak solutions to  $\text{VI}[F_{\omega^N}, \mathcal{X}]$  are exactly the same as strong solutions: points  $\bar{x} \in \mathcal{X}$  such that  $\langle F_{\omega^N}(\bar{x}), x - \bar{x} \rangle \geq 0$  for all  $x \in \mathcal{X}$ .

<sup>2</sup>Indeed, (1) says that a particular entry in  $\beta$ ,  $\beta_k$  or  $\beta_{k\ell}^s$ , affects at most one entry in  $\eta^T(\omega_{t-d}^{t-1})\beta$ , namely, the  $k$ -th one, implying that the columns of  $\eta^T(\cdot)$  have at most one nonzero entry each.

<sup>3</sup>A vector field  $F : X \rightarrow \mathbf{R}^N$  defined on a nonempty convex subset  $X$  of  $\mathbf{R}^N$  is called *monotone*, if  $[F(x) - F(y)]^T [x - y] \geq 0$  whenever  $x, y \in X$ .

Moreover, the empirical vector field  $F_{\omega^N}(x)$  is just the gradient field of the convex quadratic function

$$\Psi_{\omega^N}(x) = \frac{1}{2N} \sum_{t=1}^N \|\eta^T(\omega_{t-d}^{t-1})x - \omega_t\|_2^2, \quad (5)$$

so that weak (which is equivalent to strong) solutions to  $\text{VI}[F_{\omega^N}, \mathcal{X}]$  are just minimizers of this function on the domain  $\mathcal{X}$ . In other words, our estimate based on solving variational inequality is the optimal solution to the Least Squares (LS) formulation: the constrained optimization problem

$$\min_{x \in \mathcal{X}} \Psi_{\omega^N}(x) \quad (6)$$

with convex quadratic objective. Problem (6), same as a general variational inequality with monotone operator, can be routinely and efficiently solved by convex optimization algorithms.

### 2.3 Performance guarantees

Observe that the vector of true parameters  $\beta$  underlying our observations not only solves variational inequality  $\text{VI}[F, \mathcal{X}]$ , but also solves the following variational inequality

$$\text{find } z \in \mathcal{X} : \langle \bar{F}_{\omega^N}(w), w - z \rangle \geq 0, \quad \forall w \in \mathcal{X}, \quad \text{VI}[\bar{F}_{\omega^N}, \mathcal{X}]$$

where

$$\bar{F}_{\omega^N}(x) = A[\omega^N]x - \underbrace{\frac{1}{N} \sum_{t=1}^N \eta(\omega_{t-d}^{t-1})\eta^T(\omega_{t-d}^{t-1})\beta}_{\bar{a}[\omega^N]};$$

with  $A[\omega^N]$  defined in (4).

In fact,  $\beta$  is just a root of  $\bar{F}_{\omega^N}(x)$ :  $\bar{F}_{\omega^N}(\beta) = 0$ . Moreover, the monotone affine operators  $F_{\omega^N}(x)$  and  $\bar{F}_{\omega^N}(x)$  differ only in the value of constant term: in  $F_{\omega^N}$  this term is  $a[\omega^N]$ , and in  $\bar{F}_{\omega^N}$  this term is  $\bar{a}[\omega^N]$ . Thus, equivalently,  $\beta$  is the minimizer on  $\mathcal{X}$  of the quadratic form

$$\bar{\Psi}_{\omega^N}(x) := \frac{1}{2N} \sum_{t=1}^N \|\eta^T(\omega_{t-d}^{t-1})x - \eta^T(\omega_{t-d}^{t-1})\beta\|_2^2,$$

and the functions  $\Psi$  and  $\bar{\Psi}$  differ only in the constant terms (which do not affect the results of minimization) and in the linear terms; the difference of the vectors of coefficients of linear terms is given by (due to  $\bar{F}_{\omega^N}(\beta) = 0$ ):

$$\Delta_F := F_{\omega^N}(\beta) - \bar{F}_{\omega^N}(\beta) = F_{\omega^N}(\beta) = \bar{a}[\omega^N] - a[\omega^N] = \frac{1}{N} \sum_{t=1}^N \underbrace{\eta(\omega_{t-d}^{t-1})[\eta^T(\omega_{t-d}^{t-1})\beta - \omega_t]}_{\xi_t}. \quad (7)$$

Note that this is the same as the difference of constant terms in  $F_{\omega^N}(\cdot)$  and  $\bar{F}_{\omega^N}(\cdot)$ .

Since the conditional expectation of  $\omega_t$  given  $\omega^{t-1}$  is  $\eta^T(\omega_{t-d}^{t-1})\beta$ , we have  $\mathbf{E}_{\omega_t|\omega^{t-1}}[\xi_t] = 0$ . Thus, the right hand side in (7) is *martingale-difference*. Also, since both  $\omega_t$  and  $\eta^T(\omega_{t-d}^{t-1})\beta$  are vectors with nonnegative entries not exceeding 1, we have  $\|\eta^T(\omega_{t-d}^{t-1})\beta - \omega_t\|_\infty \leq 1$ . Besides this,  $\eta(\omega_{t-d}^{t-1})$  is a Boolean matrix with at most one nonzero in every row, whence  $\|\eta(\omega_{t-d}^{t-1})z\|_\infty \leq \|z\|_\infty$  for all  $z$ . The bottom line is that  $\|\xi_t\|_\infty \leq 1$ . As a result, we obtain

**Lemma 1** (Bounding deviation). *The  $\ell_\infty$  norm of  $F_{\omega^N}(\beta) = \Delta_F$  in (7) can be bounded as follows*

$$\text{Prob}_{\omega^N} \left\{ \|F_{\omega^N}(\beta)\|_\infty > \gamma/\sqrt{N} \right\} \leq 2\kappa \exp\{-\gamma^2/2\}, \quad \forall \gamma \geq 0. \quad (8)$$

*Proof.* Denoting by  $\mathbf{E}_{|\omega^t}$  the conditional expectation given  $\omega^t$ , for  $\gamma \geq 0$  and  $i = 1, \dots, \kappa$ , we have

$$\begin{aligned} \mathbf{E}_{\omega^{t+1}} \left\{ \exp\left\{ \sum_{s=1}^{t+1} \gamma[\xi_s]_i \right\} \right\} &= \mathbf{E}_{\omega^t} \left\{ \exp\left\{ \sum_{s=1}^t \gamma[\xi_s]_i \right\} \mathbf{E}_{\omega^{t+1}|\omega^t} \left\{ \exp\{\gamma[\xi_{t+1}]_i\} \right\} \right\} \\ &\leq \mathbf{E}_{\omega^t} \left\{ \exp\left\{ \sum_{s=1}^t [\xi_s]_i \right\} \exp\{\gamma^2/2\} \right\}, \end{aligned}$$

where the last equality is due to the Hoeffding's inequality and the fact that the conditional,  $\omega^t$  given, distribution of  $[\xi_{t+1}]_i$  is zero mean and is supported on  $[-1, 1]$ . By induction, we have

$$\mathbf{E}_{\omega^N} \left\{ \exp\left\{ \gamma \left[ \sum_{t=1}^N \xi_t \right]_i \right\} \right\} \leq \exp\{N\gamma^2/2\},$$

Now using Chernoff bound, we have

$$\text{Prob}_{\omega^N} \left\{ \frac{1}{N} \left[ \sum_{t=1}^N \xi_t \right]_i > \theta \right\} \leq \exp\{-\mu\theta\} \mathbf{E}_{\omega^N} \left\{ \exp\left\{ \mu \frac{1}{N} \left[ \sum_{t=1}^N \xi_t \right]_i \right\} \right\} \leq \exp\left\{-\mu\theta + \frac{\mu^2}{2N}\right\}.$$

Setting  $\theta = \gamma/\sqrt{N}$  and  $\mu = N\theta$ , we get  $\text{Prob}_{\omega^N} \left\{ \frac{1}{N} \left[ \sum_{t=1}^N \xi_t \right]_i > \gamma/\sqrt{N} \right\} \leq \exp\{-\gamma^2/2\}$ . The same reasoning applied to  $-\xi_t$ 's in the role of  $\xi_t$ 's results in  $\text{Prob}_{\omega^N} \left\{ \frac{1}{N} \left[ \sum_{t=1}^N \xi_t \right]_i < -\gamma/\sqrt{N} \right\} \leq \exp\{-\gamma^2/2\}$ . These inequalities combine with the union bound to imply (8).  $\square$

We are about to extract from this lemma upper bounds on the accuracy of our recovered coefficient.

### 2.3.1 Upper-bounding risk

Recall that our estimate  $\hat{\beta} := \hat{\beta}(\omega^N)$  solves the variational inequality  $\text{VI}[F_{\omega^N}, \mathcal{X}]$  with  $F_{\omega^N}(x) = A[\omega^N]x - a[\omega^N]$ , see (4). Note that  $A[\omega^N]$  is positive semidefinite. Below, we write  $A \succeq 0$  and  $A \succ 0$  to express that  $A$  is positive semidefinite and positive definite, respectively. Given  $A \in \mathbf{R}^{\kappa \times \kappa}$ ,  $A \succeq 0$ , and  $p \in [1, \infty]$ , define the “condition number”

$$\theta_p[A] := \max \left\{ \theta \geq 0 : g^T A g \geq \theta \|g\|_p^2, \quad \forall g \in \mathbf{R}^\kappa \right\}. \quad (9)$$

Observe that  $\theta_p[A] > 0$  whenever  $A \succ 0$ , and that for  $p, p' \in [0, \infty]$  one has

$$g^T A g \geq \frac{1}{2} \left\{ \theta_p[A] \|g\|_p^2 + \theta_{p'}[A] \|g\|_{p'}^2 \right\} \geq \sqrt{\theta_p[A] \theta_{p'}[A]} \|g\|_p \|g\|_{p'}. \quad (10)$$

The following observation is immediate:



**Theorem 2** (Bounding  $\ell_p$  estimation error). *For every  $p \in [1, \infty]$  and every  $\omega^N$  one has*

$$\|\widehat{\beta}(\omega^N) - \beta\|_p \leq \|F_{\omega^N}(\beta)\|_\infty / \sqrt{\theta_p[A[\omega^N]]\theta_1[A[\omega^N]]}. \quad (11)$$

*As a result, for every  $\epsilon \in (0, 1)$ , the probability of the event*

$$\|\widehat{\beta}(\omega^N) - \beta\|_p \leq \frac{\sqrt{2\ln(2\kappa/\epsilon)}}{\sqrt{\theta_p[A[\omega^N]]\theta_1[A[\omega^N]]}\sqrt{N}}, \quad \forall p \in [1, \infty] \quad (12)$$

*is at least  $1 - \epsilon$ .*

*Proof.* Let us fix  $\omega^N$  and set  $\widehat{\beta} = \widehat{\beta}[\omega^N]$ ,  $F(\cdot) = F_{\omega^N}(\cdot)$ ,  $A = A[\omega^N]$ ,  $\Delta = \beta - \widehat{\beta}$ . Since  $F(\cdot)$  is continuous and  $\widehat{\beta}$  is a weak solution to  $\text{VI}[F, \mathcal{X}]$ ,  $\widehat{\beta}$  is a strong solution to this variational inequality:  $\langle z - \widehat{\beta}, F(\widehat{\beta}) \rangle \geq 0$  for all  $z \in \mathcal{X}$ . In particular,  $\langle F(\widehat{\beta}), \Delta \rangle \geq 0$ . On the other hand,  $F(\widehat{\beta}) = F(\beta) - A\Delta$ . As a result,  $0 \leq \langle F(\widehat{\beta}), \Delta \rangle = \langle F(\beta) - A\Delta, \Delta \rangle$ , whence

$$\Delta^T A \Delta \leq \langle F(\beta), \Delta \rangle \leq \|F(\beta)\|_\infty \|\Delta\|_1. \quad (13)$$

By setting  $p' = 1$  in (10), we have  $\Delta^T A \Delta \geq \sqrt{\theta_1[A]\theta_{p'}[A]}\|\Delta\|_1\|\Delta\|_{p'}$ , this combines with (13) to imply (11); (11) combines with (8) to imply (12).  $\square$

**Remark 1** (Evaluating the condition number). *To make the upper bound (12) useful, one needs to know how to compute the “condition numbers”  $\theta_p[A]$  for a positive definite matrix  $A$ . The computation is easy when  $p = 2$ , in which case  $\theta_2[A]$  is the minimal eigenvalue of  $A$ , and when  $p = \infty$ :*

$$\theta_\infty[A] = \min_{1 \leq i \leq \kappa} \{x^T A x : \|x\|_\infty \leq 1, x_i = 1\}$$

*is the minimum of  $\kappa$  efficiently computable quantities. In general,  $\theta_1[A]$  is difficult to compute, but this quantity admits an efficiently computable tight within the factor  $\pi/2$  lower bound. Specifically, this can be done as follows. For a symmetric positive definite  $A$ ,  $\min_z \{z^T A z : \|z\|_1 = 1\}$  is the largest  $r > 0$  such that the ellipsoid  $\{z : z^T A z \leq r\}$  is contained in the unit  $\|\cdot\|_1$ -ball, or, passing to polars, the largest  $r$  such that the ellipsoid  $y^T A^{-1} y \leq r^{-1}$  contains the unit  $\|\cdot\|_\infty$ -ball. Because of this, the definition of  $\theta_1[A]$  in (9) is equivalent to  $\theta_1[A] = [\max_{\|x\|_\infty \leq 1} x^T A^{-1} x]^{-1}$ . It remains to note that when  $Q$  is a symmetric positive semidefinite  $\kappa \times \kappa$  matrix, the efficiently computable semidefinite relaxation upper bound on  $\max_{\|x\|_\infty \leq 1} x^T Q x$ , given by*

$$\min_{\lambda} \left\{ \sum_i \lambda_i : \lambda_i \geq 0, \forall i; \text{Diag}\{\lambda_1, \dots, \lambda_\kappa\} \succeq Q \right\},$$

*is tight within the factor  $\pi/2$ , see [12].*

### 2.3.2 Confidence intervals for linear forms of $\beta$

We can use Lemma 1 to build confidence intervals for linear functionals of  $\beta$ . Consider a linear form of  $\beta$ ,  $e^T \beta$ , with an arbitrary vector  $e \in \mathbb{R}^\kappa$ . Consider the pair of optimization problems

$$\begin{aligned} \underline{e}[\omega^N, \epsilon] &= \min_{x \in \mathcal{X}} \left\{ e^T x : x \in \mathcal{X}, \|A[\omega^N]x - a[\omega^N]\|_\infty \leq \sqrt{2\ln(2\kappa/\epsilon)}/\sqrt{N} \right\}, \\ \bar{e}[\omega^N, \epsilon] &= \max_{x \in \mathcal{X}} \left\{ e^T x : x \in \mathcal{X}, \|A[\omega^N]x - a[\omega^N]\|_\infty \leq \sqrt{2\ln(2\kappa/\epsilon)}/\sqrt{N} \right\}, \end{aligned} \quad (14)$$

where the parameter  $\epsilon$  varies in  $(0, 1)$ . These problems clearly are convex, so that  $\underline{e}[\omega^N, \epsilon]$  and  $\bar{e}[\omega^N, \epsilon]$  are efficiently computable. Immediately, we have the following

**Lemma 3.** *Given reliability tolerance  $\epsilon \in (0, 1)$ , the probability of the event*

$$\underline{e}[\omega^N, \epsilon] \leq e^T \beta \leq \bar{e}[\omega^N, \epsilon], \quad \forall e, \quad (15)$$

*is at least  $1 - \epsilon$ .*

Indeed, when the event  $\|\Delta_F\|_\infty \leq \sqrt{2 \ln(2\kappa/\epsilon)}/\sqrt{N}$  takes place,  $\beta$  is a feasible solution to every one of the optimization problems in (14). This implies that (15), and the event in question, due to Lemma 1, takes place with probability at least  $1 - \epsilon$ . Note that when  $e$  in (15) is a standard basis, we obtain a confidence interval for individual coefficient of  $\beta$ .

Under favorable circumstances, we can expect that for large  $N$ , the minimal eigenvalue of  $A[\omega^N]$  will be of order of 1 with overwhelming probability. This implies that the lengths of the confidence intervals (15) will go to 0 as  $N \rightarrow \infty$  at the rate  $O(1/\sqrt{N})$ . Note, however, that inter-dependence of the “regressors”  $\eta(\omega_{t-d}^{t-1})$  across  $t$  makes it very difficult to prove something along these lines.

## 2.4 Extensions: Recovery for multi-state spatio-temporal processes

In this section, we consider the multi-state spatio-temporal process. This formulation will enable us to consider marked spatial-temporal process [11], where each event outcome will contain additional information about its category. For the time being, we considered the case where at every time instant  $t$  the state of every location  $k$  is either  $\omega_{tk} = 0$  (“no event”), or  $\omega_{tk} = 1$  (“event”). We can extend our model by allowing the state of a location at a time instant to take  $M \geq 2$  “nontrivial” values on the top of the zero value “no event.” Different from the single-state observation, the multi-state observations at each time, the observation can be categorical (we can either observe no event, or observe an event of  $M$  possible outcomes.)

Let us define  $M$ -state spatio-temporal process with memory depth  $d$  as follows:

- We observe a random process on time horizon  $\{t : -d + 1 \leq t \leq N\}$ , observation at time  $t$  being

$$\omega_t = \{\omega_{tk} \in \{0, 1, \dots, M\}, 1 \leq k \leq K\}.$$

- For every  $t \geq 1$ , the conditional,  $\omega^{t-1} = (\omega_{-d+1}, \omega_{-d+2}, \dots, \omega_{t-1})$  given, distribution of  $\omega_{tk}$  is defined as follows. With every location  $k$ , the nature associates an array of true parameters  $\beta_k = \{\beta_k(p), 1 \leq p \leq M\}$ , and with every pair of locations  $k, \ell$  and every  $s \in \{1, \dots, d\}$  it associates an array of true parameters  $\beta_{k\ell}^s = \{\beta_{k\ell}^s(p, q), 1 \leq p \leq M, 0 \leq q \leq M\}$ . The induced by  $\omega^{t-1}$  probability of  $\omega_{tk}$  to be of category  $p$ ,  $1 \leq p \leq M$ , is given by

$$\beta_k(p) + \sum_{s=1}^d \sum_{\ell=1}^K \beta_{k\ell}^s(p, \omega_{(t-s)\ell}), \quad (16)$$

and the probability for  $\omega_{tk}$  to take value 0 is the complement to 1 of the sum of quantities (16) over  $p = 1, \dots, M$ . In other words,  $\beta_{k\ell}^s(p, q)$  is the contribution of the location  $\ell$  in state  $q \in \{0, 1, \dots, M\}$  at time  $t - s$  to the probability for the location  $k$  to be in state  $p \in \{1, \dots, M\}$ , at time  $t$ , and  $\beta_k(p)$ ,  $p \in \{1, \dots, M\}$  is the “endogenous” component of the probability of the latter event.

Of course, for this description to make sense, the  $\beta$ -parameters should guarantee that for every  $\omega^{t-1}$ , that is, for every collection  $\{\omega_{\tau\ell} \in \{0, 1, \dots, M\} : \tau < t, 1 \leq \ell \leq K\}$ , the prescribed by (16)

probabilities are nonnegative and their sum over  $p = 1, \dots, M$  is  $\leq 1$ . Thus, the  $\beta$ -parameters should satisfy the system of constraints

$$\begin{aligned} 0 &\leq \beta_k(p) + \sum_{s=1}^d \sum_{\ell=1}^K \min_{0 \leq q \leq M} \beta_{k\ell}^s(p, q), \quad 1 \leq p \leq M, 1 \leq k \leq K, \\ 1 &\geq \sum_{p=1}^{M-1} \beta_k(p) + \sum_{s=1}^d \sum_{\ell=1}^K \max_{0 \leq q \leq M} \sum_{p=1}^M \beta_{k\ell}^s(p, q), \quad 1 \leq k \leq K. \end{aligned} \quad (17)$$

The solution set  $\mathcal{B}$  of this system is a polyhedral set given by explicit polyhedral representations.

- We are given convex compact set  $\mathcal{X}$  in the space of parameters  $\beta = \{\beta_k, \beta_{k\ell}^s(p, q), 1 \leq s \leq d, 1 \leq k, \ell \leq K, 1 \leq p \leq M, 0 \leq q \leq M\}$  such that  $\mathcal{X}$  contains the true parameter  $\beta$  of the process we are observing, and  $\mathcal{X}$  is contained in the polytope  $\mathcal{B}$  given by constraints (17).

We arrange the collection of  $\beta$ -parameters associated with a  $M$ -state spatio-temporal process with memory depth  $d$  into a column vector (still denoted  $\beta$ ) and denote by  $\kappa$  the dimension of  $\beta$ .<sup>4</sup> Note that (16) says that the  $M$ -dimensional vector of conditional,  $\omega^{t-1}$  given, probabilities for  $\omega_{tk}$  to take values  $p \in \{1, \dots, M\}$  is

$$[\eta_k^T(\omega_{t-d}^{t-1})\beta]_p$$

with known to us function  $\eta_k(\cdot)$  defined on the set of all arrays  $\omega^N = \{\omega_{\tau k} \in \{0, 1, \dots, M\}, 1 \leq \tau \leq d, 1 \leq k \leq K\}$  and taking values in the space of  $\kappa \times M$  matrices. Note that the value of  $\omega_{tk}$  is the index of the category, and does not mean magnitude. Also note that  $\eta_k(\omega_{t-d}^{t-1})$  is a Boolean matrix.

To proceed, for  $0 \leq q \leq M$ , let  $\chi_q \in \mathbf{R}^M$  be defined as follows:  $\chi_0 = 0$ , and  $\chi_q$ ,  $1 \leq q \leq M$ , is the  $q$ -th standard basis in  $\mathbf{R}^M$ . In particular, the state  $\omega_{tk}$  can be encoded by vector  $\bar{\omega}_{tk} = \chi_{\omega_{tk}}$ , and the state of our process at time  $t$  – by block vector  $\bar{\omega}_t \in \mathbf{R}^{MK}$  with blocks  $\bar{\omega}_{tk} \in \mathbf{R}^M$ ,  $k = 1, \dots, K$ . In other words: the  $k$ -th block in  $\bar{\omega}_t$  is  $M$ -dimensional vector which is  $p$ -th basic orth of  $\mathbf{R}^M$  when  $\omega_{tk} = p \geq 1$ , and is the zero vector when  $\omega_{tk} = 0$ . Arranging  $\kappa \times M$  matrices  $\eta_k(\cdot)$  into a matrix

$$\eta(\cdot) = [\eta_1(\cdot), \dots, \eta_K(\cdot)] \in \{0, 1\}^{\kappa \times MK},$$

we obtain

$$\mathbf{E}_{|\omega^{t-1}} \{\bar{\omega}_t\} = \eta^T(\omega_{t-d}^{t-1})\beta \in \mathbb{R}^{MK},$$

where  $\mathbf{E}_{|\omega^{t-1}}$  is the conditional expectation given  $\omega^{t-1}$ . Note that similarly to Section 2, (16) says that every particular entry in  $\beta$ ,  $\beta_k(p)$  or  $\beta_{k\ell}^s(p, q)$ , affects at most one of the entries in the block vector  $[\eta_1^T(\omega_{t-d}^{t-1})\beta; \dots; \eta_K^T(\omega_{t-d}^{t-1})\beta]$  specifically, the  $p$ -th entry of the  $k$ -th block, so that the Boolean matrix  $\eta(\omega_{t-d}^{t-1})$  has at most one nonzero entry in every row.

Note that the spatio-temporal Bernoulli process with memory depth  $d$ , as defined in Section 2, is a special case of single-state ( $M = 1$ ) spatio-temporal process with memory depth  $d$ , the case where state 0 at a location contributes nothing to probability of state 1 in another location at a later time, that is,  $\beta_{k\ell}^s(1, 0) = 0$  for all  $s, k, \ell$ .

**Motivating example: Different types of crime events.** An illustration to the multistate spatio-temporal model is modeling of crime events with different types, e.g., burglary and robbery. We also split the geographic area of interest into  $K$  non-overlapping cells, which will be our locations. Selecting the time step in such a way that we can ignore the chances for two or more crime events

<sup>4</sup>In general,  $\kappa = KM + dK^2M^2$ . However, depending on application, it could make sense to postulate that some of the components of  $\beta$  are zeros, thus reducing the actual dimension of  $\beta$ ; for example, we could assume that  $\beta_{k\ell}(\cdot, \cdot) = 0$  for some “definitely non-interacting” pairs  $k, \ell$  of locations.

to occur in the same spatio-temporal cell, we can model the history of crime events in the area as a  $M = 2$ -state spatio-temporal process, with additional to (17) convex restrictions on the vector of parameters  $\beta$  expressing our *a priori* information on the probability  $\beta_k(p)$  of a “newborn” crime event of category  $p$  to occur at time instant  $t$  in location  $k$  and on the contribution  $\beta_{k\ell}^s(p, q)$  of a crime event of category  $q$  in spatio-temporal cell  $\{(t-s), \ell\}$  to the probability of crime event of category  $p$ ,  $p \geq 1$ , to happen in the spatio-temporal cell  $\{t, k\}$ .

The problem of estimating parameters  $\beta$  of the  $M$ -state spatio-temporal process from observations of this process can be processed exactly as in the case of the single state spatio-temporal Bernoulli process. Specifically, observations  $\omega^N$  give rise to two monotone and affine vector fields on  $\mathcal{X}$ , the first observable and the second unobservable:

$$\begin{aligned} F_{\omega^N}(x) &= \underbrace{\left[ \frac{1}{N} \sum_{t=1}^N \eta(\omega_{t-d}^{t-1}) \eta^T(\omega_{t-d}^{t-1}) \right]}_{A[\omega^N]} - \underbrace{\frac{1}{N} \eta(\omega_{t-d}^{t-1}) \bar{\omega}_t}_{a[\omega^N]}, \\ \bar{F}_{\omega^N}(x) &= A[\omega^N]x - A[\omega^N]\beta. \end{aligned} \quad (18)$$

These two fields differ only in constant term,  $\beta$  is a root of the second field, and the difference of constant terms, or, which is the same due to  $\bar{F}_{\omega^N}(\beta) = 0$ , the vector  $F_{\omega^N}(\beta)$  is a martingale-difference satisfying, by exactly the same reasons as in Section 2, bound (8). To recover  $\beta$  from observations, we could use the Least Squares (LS) estimate obtained by solving variational inequality  $\text{VI}[F_{\omega^N}, \mathcal{X}]$  with the just defined  $F_{\omega^N}$ , or, which is the same, obtained by solving the problem

$$\min_{x \in \mathcal{X}} \left\{ \Psi_{\omega^N}(x) := \frac{1}{2N} \sum_{t=1}^N \|\eta^T(\omega_{t-d}^{t-1})x - \bar{\omega}_t\|_2^2 \right\}. \quad (19)$$

Note that (8) (which does take place in our present situation) by the same argument as in Section 2, implies the validity in our present situation of Theorem 2 and Lemma 3.

### 3 Nonlinear link function

So far our discussion has been focused on “linear” link functions, where past events contribute additively to the probability of a specific event in a specific spatio-temporal cell. Now we consider non-linear link function. This generalizes our model to allow more complex spatio-temporal interactions.

#### 3.1 Single-state process

Let  $\phi(\cdot) : D \rightarrow \mathbf{R}^K$  be a continuous *monotone* vector field defined on a closed convex domain  $D \subset \mathbf{R}^K$  such that

$$y \in D \Rightarrow 0 \leq \phi(y) \leq [1; \dots; 1].$$

For example, we can take the sigmoid function

$$[\phi(u)]_k = \frac{\exp\{u_k\}}{1 + \exp\{u_k\}}, \quad k \leq K, \quad D = \mathbf{R}^K.$$

Given positive integer  $N$ , let us define a *spatio-temporal Bernoulli process with memory depth  $d$  and link function  $\phi$*  as a random process with realizations  $\{\omega_{tk} \in \{0, 1\}, k \leq K, -d+1 \leq t \leq N\}$  by replacing assumptions from Section 2 with the assumptions that

- the vector  $\beta \in \mathbf{R}^\kappa$  of process's parameters satisfies the restrictions

$$\eta^T(\omega_{t-d}^{t-1})\beta \in D, \quad \forall 1 \leq t \leq N \quad (20)$$

with given functions  $\eta(\omega_{t-d}^{t-1})$  taking values in the space of  $\kappa \times K$  matrices;

- the conditional,  $\omega^{t-1}$  given, expectation of  $\omega_t \in \{0, 1\}^K$  is  $\phi(\eta^T(\omega_{t-d}^{t-1})\beta)$ ;
- we are given a convex compact set  $\mathcal{X}$  such that the vector of parameters  $\beta$  underlying the observed process belongs to  $\mathcal{X}$  and every  $\beta \in \mathcal{X}$  satisfies (20).

Set

$$\begin{aligned} F(x) &= \frac{1}{N} \mathbf{E}_{\omega^N} \left\{ \sum_{t=1}^N [\eta(\omega_{t-d}^{t-1})\phi(\eta^T(\omega_{t-d}^{t-1})x) - \eta(\omega_{t-d}^{t-1})\omega_t] \right\} : \mathcal{X} \rightarrow \mathbf{R}^\kappa, \\ F_{\omega^N}(x) &= \underbrace{\frac{1}{N} \sum_{t=1}^N \eta(\omega_{t-d}^{t-1})\phi(\eta^T(\omega_{t-d}^{t-1})x)}_{A_{\omega^N}(x)} - \underbrace{\frac{1}{N} \sum_{t=1}^N \eta(\omega_{t-d}^{t-1})\omega_t}_{a[\omega^N]} : \mathcal{X} \rightarrow \mathbf{R}^\kappa, \\ \bar{F}_{\omega^N}(x) &= A_{\omega^N}(x) - \underbrace{\frac{1}{N} \sum_{t=1}^N \eta(\omega_{t-d}^{t-1})\phi(\eta^T(\omega_{t-d}^{t-1})\beta)}_{\bar{a}[\omega^N]} : \mathcal{X} \rightarrow \mathbf{R}^\kappa. \end{aligned} \quad (21)$$

Then we find ourselves basically in the same situation as in Section 2 (in fact, in Section 2, we were speaking about the special case  $\phi(z) \equiv z$  of our present situation).

Specifically,  $F(\cdot)$  is a monotone (albeit not affine anymore) vector field on  $\mathcal{X}$ ,  $F(\beta) = 0$ . The empirical version  $F_{\omega^N}(x)$ , for every  $x \in \mathcal{X}$ , is a monotone on  $\mathcal{X}$  vector field which is an unbiased estimate of  $F(x)$ . Besides this,  $\bar{F}_{\omega^N}(x)$  is a monotone on  $\mathcal{X}$  vector field, and the true vector of parameters  $\beta$  underlying our observations solves the variational inequality  $\text{VI}[\bar{F}_{\omega^N}, \mathcal{X}]$ , moreover, is a root of the vector field  $\bar{F}_{\omega^N}$ . These observations suggest estimating  $\beta$  by weak solution to the variational inequality  $\text{VI}[F_{\omega^N}, \mathcal{X}]$ .

Note that same as before, the vector fields  $F_{\omega^N}$  and  $\bar{F}_{\omega^N}$  differ only in the constant terms, and the difference of these constant terms is nothing but  $F_{\omega^N}(\beta)$  due to  $\bar{F}_{\omega^N}(\beta) = 0$ . Moreover, the difference of these constant terms is a martingale-difference. While probabilities of large deviations for this martingale-difference do not obey the same bound as in the case of  $\phi(z) \equiv z$  (since the matrices  $\eta(\omega_{t-d}^{t-1})$  now not necessarily are Boolean with at most one nonzero in a row), the reasoning which led us to (8) demonstrates that the vector  $F_{\omega^N}(\beta)$  in our present situation does obey the bound

$$\text{Prob}_{\omega^N} \left\{ \|F_{\omega^N}(\beta)\|_\infty > \gamma \Theta \sqrt{N} \right\} \leq 2\kappa \exp\{-\gamma^2/2\}, \quad \forall \gamma \geq 0, \quad (22)$$

where  $\Theta$  is the maximum, over the rows of  $\eta(\omega_{t-d}^{t-1})$  and  $\omega_{d-1}^{t-1}$ , of  $\|\cdot\|_1$ -norms of the rows. Note that in the situation of this section, our  $O(1/\sqrt{N})$  exponential bounds on large deviations of  $F_{\omega^N}(\beta)$  from zero, while being a good news, do *not* result in easy-to-compute on-line upper risk bounds and confidence intervals for linear functions of  $\beta$ . Indeed, to adjust to our present situation Theorem 2, we need to replace the condition numbers  $\theta_p[\cdot]$  with constants of strong monotonicity of the vector field  $F_{\omega^N}(\cdot)$  on  $\mathcal{X}$ , and to adjust Lemma 3, we need to replace the quantities  $\bar{e}$  and  $\underline{e}$ , see (14), with the maximum (resp., minimum) of linear form over the set  $\{x \in \mathcal{X} : \|F_{\omega^N}(x)\|_\infty \leq \delta\}$ . Both these tasks for a *nonlinear* operator  $F_{\omega^N}(\cdot)$  seem to be highly problematic.

### 3.2 Multi-state processes

We can extend the construction from the previous item to  $M$ -state processes. Below with a slight abuse of notation without causing confusion, we will re-define and re-use notations for the multi-state processes.

Let us identify two-dimensional  $K \times M$  array  $\{a_{k\ell} : 1 \leq k \leq K, 1 \leq \ell \leq M\}$  with  $KM$ -dimensional block vector with  $K$  blocks  $[a_{k1}; a_{k2}; \dots; a_{kM}]$ ,  $1 \leq k \leq K$ , of dimension  $M$  each. With this convention, a parametric  $K \times M$  array  $\psi(z) = \{\psi_{kp}(z) \in \mathbf{R} : k \leq K, 1 \leq p \leq M\}$  depending on  $KM$ -dimensional vector  $z$  of parameters becomes a vector field on  $\mathbf{R}^{KM}$ . Assume that we are given an array  $\phi(\cdot) = \{\phi_{kp}(\cdot) \in \mathbf{R} : k \leq K, 1 \leq p \leq M\}$ , of the structure just outlined, such that the vector field  $\phi(\cdot)$  is continuous and monotone on a closed convex domain  $D \subset \mathbf{R}^{KM}$ , and

$$y \in D \Rightarrow 0 \leq \phi(y) \leq 1, \quad \sum_{p=1}^M \phi_{kp}(y) \leq 1, \quad 1 \leq k \leq K. \quad (23)$$

Now, we assume that the conditional,  $\omega^{t-1}$  given, probability for location  $k$  at time  $t$  to be at state  $p \in \{1, \dots, M\}$  (i.e., to have  $\omega_{tk} = p$ ) is

$$\phi_{kp}(\eta^T(\omega_{t-d}^{t-1})\beta)$$

for some vector of parameters  $\beta \in \mathbf{R}^\kappa$  and known to us function  $\eta(\cdot)$  taking values in the space of  $\kappa \times KM$  matrices and such that  $\eta^T(\omega_{t-d}^{t-1})\beta \in D$  whenever  $\omega_{\tau k} \in \{0, 1, \dots, M\}$  for all  $\tau$  and  $k$ . As a result, the conditional,  $\omega^{t-1}$  given, probability to have  $\omega_{tk} = 0$  is

$$1 - \sum_{p=1}^M \phi_{kp}(\eta^T(\omega_{t-d}^{t-1})\beta).$$

In addition, we assume that we are given a convex compact set  $\mathcal{X} \subset \mathbf{R}^\kappa$  such that  $\beta \in \mathcal{X}$  and

$$\beta \in \mathcal{X} \Rightarrow \eta^T(\omega_{t-d}^{t-1})\beta \in D, \quad \forall \{\omega_{\tau k} \in \{0, 1, \dots, M\}, \forall \tau, k\}.$$

Same as in Section 2.4, we can encode the collection  $\{\omega_{tk} : 1 \leq k \leq K\}$  of locations' states at time  $t$  by block vector  $\bar{\omega}_t$  with  $K$  blocks of dimension  $M$  each, with  $k$ -th block equal to  $\omega_{tk}$ -th basic standard basis in  $\mathbf{R}^M$  when  $\omega_{tk} > 0$  and equal to 0 when  $\omega_{tk} = 0$ . We clearly have

$$\mathbf{E}_{|\omega^{t-1}} \{\bar{\omega}_t\} = \phi(\eta^T(\omega_{t-d}^{t-1})\beta).$$

Setting

$$\begin{aligned} F(x) &= \frac{1}{N} \mathbf{E}_{\omega^N} \left\{ \sum_{t=1}^N [\eta(\omega_{t-d}^{t-1})\phi(\eta_t^T(\omega_{t-d}^{t-1})x) - \eta(\omega_{t-d}^{t-1})\bar{\omega}_t] \right\} : \mathcal{X} \rightarrow \mathbf{R}^\kappa, \\ F_{\omega^N}(x) &= \underbrace{\frac{1}{N} \sum_{t=1}^N \eta(\omega_{t-d}^{t-1})\phi(\eta_t^T(\omega_{t-d}^{t-1})x)}_{A_{\omega^N}(\beta)} - \underbrace{\frac{1}{N} \sum_{t=1}^N \eta(\omega_{t-d}^{t-1})\bar{\omega}_t}_{a[\omega^N]} : \mathcal{X} \rightarrow \mathbf{R}^\kappa \\ \bar{F}_{\omega^N}(x) &= A_{\omega^N}(x) - \underbrace{\frac{1}{N} \sum_{t=1}^N \eta(\omega_{t-d}^{t-1})\phi(\eta_t^T(\omega_{t-d}^{t-1})x)}_{\bar{a}[\omega^N]} : \mathcal{X} \rightarrow \mathbf{R}^\kappa, \end{aligned} \quad (24)$$

(cf. equation (21)), we can repeat word by word everything stated at the end of previous item.

## 4 Maximum Likelihood estimate

In the previous sections, we have discussed recovery by Least Squares (LS) estimate. In this section, we will consider an alternative approach based on the Maximum Likelihood (ML) estimate, which is commonly used in statistics. ML estimate is obtained by maximizing over  $\beta \in \mathcal{X}$  the conditional likelihood of what we have observed, the condition being the actually observed values of  $\omega_{tk}$  for  $-d+1 \leq t \leq 0$  and  $1 \leq k \leq K$ . In this section, we study the property of the ML estimate and show that it corresponds to a convex optimization problem.

### 4.1 ML estimate for single and multi-state

**Single state.** Assume, in addition to what has been already assumed, that for every  $t$  the random variables  $\omega_{tk}$  are conditionally independent across  $k$  given  $\omega^{t-1}$ . Then the negative log-likelihood, conditioned by the value of  $\omega^0$ , is given by

$$L(\beta) = \frac{1}{N} \sum_{t=1}^N \sum_{k=1}^K \left[ -\omega_{tk} \ln \left( \beta_k + \sum_{s=1}^d \sum_{\ell=1}^K \beta_{k\ell}^s \omega_{(t-s)\ell} \right) - (1 - \omega_{tk}) \ln \left( 1 - \beta_k - \sum_{s=1}^d \sum_{\ell=1}^K \beta_{k\ell}^s \omega_{(t-s)\ell} \right) \right],$$

which is a convex function. So the ML estimate in our model reduces to the convex program

$$\min_{\beta \in \mathcal{X}} L(\beta). \quad (25)$$

**Multiple states.** Assume the states of locations  $k$  at time  $t$  are conditionally,  $\omega^{t-1}$  given, independent across  $k \leq M$ . Then the ML estimate is given by minimizing, over  $\beta \in \mathcal{X}$ , the conditional negative log-likelihood of our collection  $\omega^N$  of observations (the condition being the initial segment  $\omega^0$  of the observation). The objective in this minimization problem is the convex function (after scaling the negative log-likelihood by  $1/N$ ):

$$L_{\omega^N}(\beta) = -\frac{1}{N} \sum_{t=1}^N \sum_{k=1}^K \psi_{tk}^{\omega^N}(\beta),$$

where

$$\psi_{tk}^{\omega^N}(\beta) = \begin{cases} \ln \left( [\eta_k^T(\omega_{t-d}^{t-1})\beta]_{\omega_{tk}} \right), & \omega_{tk} \in \{1, \dots, M\}, \\ \ln \left( 1 - \sum_{\iota=1}^M [\eta_k^T(\omega_{t-d}^{t-1})\beta]_{\iota} \right), & \omega_{tk} = 0. \end{cases} \quad (26)$$

### 4.2 Performance guarantee

We are about to show that the ML estimate has structure similar to the LS estimator that we have dealt with earlier, and obeys bounds similar to (22). Given a small positive tolerance  $\varrho$ , consider  $M$ -state spatio-temporal process with  $K$  locations and vector of parameters, as defined in Section 2.4,  $\beta \in \mathbf{R}^\kappa$  restricted to reside in the polyhedral set  $B_\varrho$  cut off  $\mathbf{R}^\kappa$  by “ $\varrho$ -strengthened” version of the constraints (17), specifically, by the constraints

$$\begin{aligned} \varrho &\leq \beta_k(p) + \sum_{s=1}^d \sum_{\ell=1}^K \min_{0 \leq q \leq M} \beta_{k\ell}^s(p, q), \quad 1 \leq p \leq M, 1 \leq k \leq K, \\ 1 - \varrho &\geq \sum_{p=1}^{M-1} \beta_k(p) + \sum_{s=1}^d \sum_{\ell=1}^K \max_{0 \leq q \leq M} \sum_{p=1}^M \beta_{k\ell}^s(p, q), \quad 1 \leq k \leq K. \end{aligned} \quad (27)$$

The purpose of strengthening the constraints on  $\beta$  is to make the maximum likelihood, to be defined below, continuously differentiable on the given to us domain of parameters.

In what follows, we treat vectors from  $\mathbf{R}^{KM}$  as block vectors with  $K$  blocks of dimension  $M$  each. For such a vector  $z$ ,  $[z]_{kp}$  stands for  $p$ -th entry in  $k$ -th block of  $z$ . Let

$$Z_0 = \{\omega \in \mathbf{R}^{MK} : \omega \geq 0, \sum_{p=1}^M [\omega]_{kp} \leq 1, \forall k \leq K\}.$$

Similarly, define

$$Z_\varrho = \{z \in \mathbf{R}^{MK} : [z]_{kp} \geq \varrho, \forall k, p, \sum_{p=1}^M [z]_{kp} \leq 1 - \varrho, \forall k\} \subset Z_0.$$

We associate with a vector  $w \in Z_0$  the convex function  $\mathcal{L}_w : Z_\varrho \rightarrow \mathbf{R}$ :

$$\mathcal{L}_w(z) := -\sum_{k=1}^K \left[ \sum_{p=1}^M [w]_{kp} \ln([z]_{kp}) + [1 - \sum_{p=1}^M [w]_{kp}] \ln(1 - \sum_{p=1}^M [z]_{kp}) \right]. \quad (28)$$

From now on, assume that we are given a convex compact set  $\mathcal{X} \subset B_\varrho$  known to contain the true vector  $\beta$  of parameters. Then the problem of minimizing the negative log-likelihood as defined in Section 4 for the multi-state case becomes

$$\min_{x \in \mathcal{X}} \left\{ L_{\omega^N}(x) = \frac{1}{N} \sum_{t=1}^N \mathcal{L}_{\bar{\omega}_t}(\eta^T(\omega_{t-d}^{t-1})x) \right\}, \quad (29)$$

where  $\bar{\omega}_t = \bar{\omega}_t(\omega^t)$  encodes, as explained in Section 2.4, the observations of time  $t$ , and  $\eta(\omega_{t-d}^{t-1})$  are the same matrix-valued functions as in Section 2.4.

Note that by construction,  $\bar{\omega}_t$  belongs to  $Z_0$ . Moreover, by construction, we have  $\eta(\omega_{t-d}^{t-1})x \in Z_\varrho$  whenever  $x \in B_\varrho$  and  $\omega_{sp} \in \{0, 1, \dots, M\}$  for all  $s, p$ . Now, minimizers of  $L_{\omega^N}(x)$  over  $x \in \mathcal{X}$  are exactly the solutions of the variational inequality stemming from  $\mathcal{X}$  and the monotone and smooth vector field (the smoothness property is due to  $L_{\omega^N}(x)$  being convex and smooth on  $\mathcal{X}$ ):

$$\begin{aligned} F_{\omega^N}(x) &= \nabla_x L_{\omega^N}(x) = \frac{1}{N} \sum_{t=1}^N \eta(\omega_{t-d}^{t-1}) \phi_{\bar{\omega}_t(\omega^t)}(\eta^T(\omega_{t-d}^{t-1})x), \\ \phi_w(z) &= \nabla_z \mathcal{L}_w(z) = -\frac{1}{N} \sum_{k=1}^K \left[ \sum_{p=1}^M \frac{[w]_{kp}}{[z]_{kp}} e^{kp} - \frac{1 - \sum_{p=1}^M [w]_{kp}}{1 - \sum_{p=1}^M [z]_{kp}} \sum_{p=1}^M e^{kp} \right], \quad [w \in Z_0] \end{aligned} \quad (30)$$

where  $e^{kp} \in \mathbf{R}^{KM}$  is the block-vector with the standard  $p$ -th standard basis in  $\mathbf{R}^M$  as the  $k$ -th block and all other blocks equal to 0.

Note that we clearly have

$$w \in Z_\varrho \Rightarrow \phi_w(w) = 0. \quad (31)$$

Let us show that  $F_{\omega^N}(\beta)$  is “typically small”: its magnitude obeys the large deviation bounds similar to (8), (22). Indeed, let us set  $\bar{z}_t(\omega^{t-1}) = \eta^T(\omega_{t-d}^{t-1})\beta$ , so that  $\bar{z}_t \in Z_\varrho$  due to  $\beta \in B_\varrho$ . Invoking (31) with  $w = \bar{z}_t(\omega^{t-1})$ , we have

$$\begin{aligned} F_{\omega^N}(\beta) &= \frac{1}{N} \sum_{t=1}^N \underbrace{\eta(\omega_{t-d}^{t-1}) \delta_t[\omega^t]}_{\xi_t}, \\ \delta_t[\omega^t] &= -\sum_{k=1}^K \left[ \sum_{p=1}^M \frac{[\bar{\omega}_t(\omega^t)]_{kp} - [\bar{z}_t(\omega^{t-1})]_{kp}}{[\bar{z}_t(\omega^{t-1})]_{kp}} e^{kp} + \frac{\sum_{p=1}^M [\bar{z}_t]_{kp} - [\bar{\omega}_t(\omega^t)]_{kp}}{1 - \sum_{p=1}^M [\bar{z}_t(\omega^{t-1})]_{kp}} \sum_{p=1}^M e^{kp} \right]. \end{aligned}$$



Since the conditional expectation of  $[\bar{\omega}_t(\omega^t)]_{kp}$  given  $\omega^{t-1}$  equals  $[\bar{z}_t(\omega^{t-1})]_{kp}$ , and the conditional expectation of  $\xi_t$  given  $\omega^{t-1}$  is zero. Besides this, random vectors  $\xi_t$  take their values in a bounded set (of size depending on  $\varrho$ ). As a result,  $\|F_{\omega^N}(\beta)\|_\infty$  admits bound on probabilities of large deviations of the form (22), with properly selected (and depending on  $\varrho$ ) factor  $\Theta$ . Unfortunately, by reasons similar to those in Section 3, it seems to be difficult to extract from this bound meaningful conclusions on the accuracy of the ML estimate.

**Remark 2** (Decomposition of LS and ML estimation). *In the models we have considered, the optimization problems we aim to solve when building the LS and the ML estimates under mild assumptions are decomposable (in spite of the fact that the observations are not i.i.d. and are dependent). Indeed, vector  $\beta = \{\beta_{kp}, \beta_{k\ell}^s(p, q), 1 \leq k, \ell \leq K, 1 \leq p \leq M, 0 \leq q \leq M, 1 \leq s \leq d\}$  of model's parameters can be split into  $K$  subvectors  $\beta^k = \{\beta_{kp}, \beta_{k\ell}^s(p, q), 1 \leq \ell \leq K, 1 \leq p \leq M, 0 \leq q \leq M, 1 \leq s \leq d\}$ ,  $k = 1, \dots, K$ . It is immediately seen that the objectives to be minimized in the problems in question are sums of  $K$  terms, with  $k$ -th term depending on  $x^k$  only. As a result, if the domain  $\mathcal{X}$  summarizing our a priori information on  $\beta$  is decomposable:  $\mathcal{X} = \{x : x^k \in \mathcal{X}_k, 1 \leq k \leq K\}$ , the optimization problems yielding the LS and the ML estimates are collections of  $K$  uncoupled convex optimization problems,  $k$ -th of them in variables  $x^k$ . Under favorable circumstances the optimization problem (6) admits even finer decomposition. Specifically, splitting  $\beta^k$  into subvectors  $\beta^{kp} = \{\beta_{kp}, \beta_{k\ell}^s(p, q), 1 \leq \ell \leq K, 1 \leq s \leq d, 0 \leq q \leq M\}$ , it is easily seen that the objective in (6) is the sum, over  $k \leq K$  and  $p \leq M$ , of functions  $\Psi_{\omega^N}^{kp}(x^{kp})$ . It follows that when  $\mathcal{X} = \{x : x^{kp} \in \mathcal{X}_{kp}, 1 \leq k \leq K, 1 \leq p \leq M\}$ , (6) is a collection of  $KM$  uncoupled convex problems  $\min_{x^{kp} \in \mathcal{X}_{kp}} \Psi_{\omega^N}^{kp}(x^{kp})$ . The outlined decompositions can be used to accelerate the solution process.*

Similar to Section 2, optimization problem (29) is decomposable, provided  $\mathcal{X}$  is so, that is,  $\mathcal{X} = \{\beta : \{\beta_{kp}, \beta_{k\ell}^s(p, q)\} \in \mathcal{X}_k, k \leq K\}$  with closed convex sets  $\mathcal{X}_k$ .

### 4.3 ML estimate with general link function

One can obtain ML estimate in the situation of nonlinear link function considered in Section 3.2. In this situation, we strengthen the restriction (23) on  $D$  to

$$y \in D \Rightarrow \varrho \leq \phi_{kp}(y) \quad \forall k, p, \quad \sum_{p=1}^M \phi_{kp}(y) \leq 1 - \varrho, \quad \forall k \quad (32)$$

with some  $\varrho > 0$ . Assuming that  $\omega_{tk}$ 's are conditionally,  $\omega^{t-1}$  given, independent across  $k$ , computing ML estimate for the general link-function reduces to solving problem (29) with  $\mathcal{L}_w(z) : D \rightarrow \mathbf{R}$ ,  $w \in Z_0$ , given by

$$\mathcal{L}_w(z) = - \sum_{k=1}^K \left[ \sum_{p=1}^M [w]_{kp} \ln(\phi_{kp}(z)) + \left[1 - \sum_{p=1}^M [w]_{kp}\right] \ln\left(1 - \sum_{p=1}^M \phi_{kp}(z)\right) \right]. \quad (33)$$

Assuming  $\phi$  continuously differentiable on  $D$  and  $\mathcal{L}_w(\cdot)$  convex on  $D$ , we can repeat, with straightforward modifications, everything what was said above (that is, in the special case of  $\phi(z) \equiv z$ ), including our exponential bounds on probabilities of large deviations of  $F_{\omega^N}(\beta)$  from zero. Note, however, that beyond the case of affine  $\phi_{kp}(\cdot)$ , the convexity of  $\mathcal{L}_w(\cdot)$  is hardly the case. This is due to the fact that the convexity on  $D$  of the functions

$$-\ln(\phi_{kp}(\cdot)), -\ln\left(1 - \sum_p \phi_{kp}(\cdot)\right)$$

is a rare commodity. Nevertheless, convexity of these functions does take place in the case of “logistic-type” link function:

$$\phi_{kp}(z) = \frac{\exp\{a_{kp}(z)\}}{\sum_{q=0}^M \exp\{a_{kq}(z)\}}$$

with functions  $a_{kq}(z)$ ,  $0 \leq q \leq M$  that are affine in  $z$ .

## 5 Simulation study

In this section, we perform multiple numerical experiments to demonstrate the good performance of the Least Square (LS) and Maximum Likelihood (ML) Estimates and show their comparisons. We present the recovery accuracy in terms of  $\ell_1$ ,  $\ell_2$ , and  $\ell_\infty$  norms for both single state and multiple states spatio-temporal Bernoulli processes, and compare the true influence function with the recoveries. Moreover, to shed insights on the possible application in causal inference [16], we show an example of the Bernoulli process based on a sparse graphical model; the recovered influence parameters match reasonably well with the underlying network structure.

### 5.1 Single state spatio-temporal processes

Here we report on a “proof of concept” experiment with the memory depth  $d = 8$  and number of locations  $K = 8$ . Here we make an additional assumption on the structure of the coefficients. The restrictions specifying  $\mathcal{X}$  (the set of possible true parameters) were expressed by the constraints that

- $\beta_k \geq 0$ ,  $\beta_{kl}^s \geq 0$ ; and  $\beta_k + \sum_{s=1}^d \sum_{\ell=1}^K \beta_{k\ell}^s \leq 1$ ,  $\forall k$ ;
- $\beta_{k\ell}^s = 0$  when  $|k - \ell| > 1$  (only neighbors can affect each other);
- For every  $1 \leq k, \ell \leq K$ ,  $\beta_{k\ell}^s$  is a *non-increasing convex* function of  $s$ .

In the experiment, we set the number of observations as  $N = 10,000$ , and the true parameter (including the baseline intensity and the influence)  $\beta$  was selected in  $\mathcal{X}$  at random. We computed the LS solution to  $\text{VI}[F_{\omega_N}, \mathcal{X}]$ , and the ML solution to (25). The observed recovery errors are presented in Table 1, and the recoveries on Figure 3.

From the numerical experiments reported in Figure 3, we observe that for recovering single-state processes, the ML and the LS estimators have comparable performances, with the ML being slightly better. The influence functions recovered from the ML and the LS are both close to the true influence function and captures its temporal decay. (In this example, we indeed has introduced a constraint for the temporal decay shape in this example.)

Table 1: Single-state process: estimation errors for ML and LS (percents: norm of recovery error in percents of the norm of true parameter vector).

Estimate	$\ell_1$ error	$\ell_2$ error	$\ell_\infty$ error
ML	1.0169 (13.38%)	0.1037 (12.62%)	0.0255 (12.16%)
LS	1.1709 (15.41%)	0.1149 (13.98%)	0.0332 (15.86%)

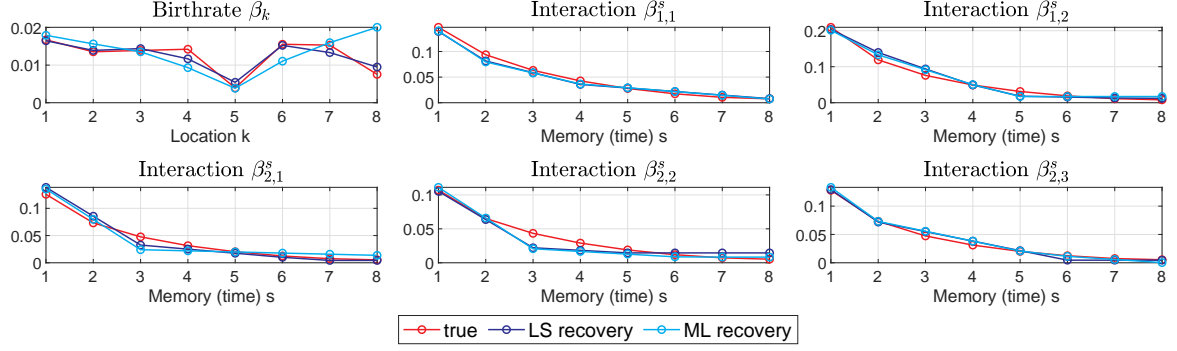


Figure 3: Single-state process: examples of LS and ML estimates for baseline intensity  $\beta_k$  and influence functions  $\beta_{k,\ell}^s$ .

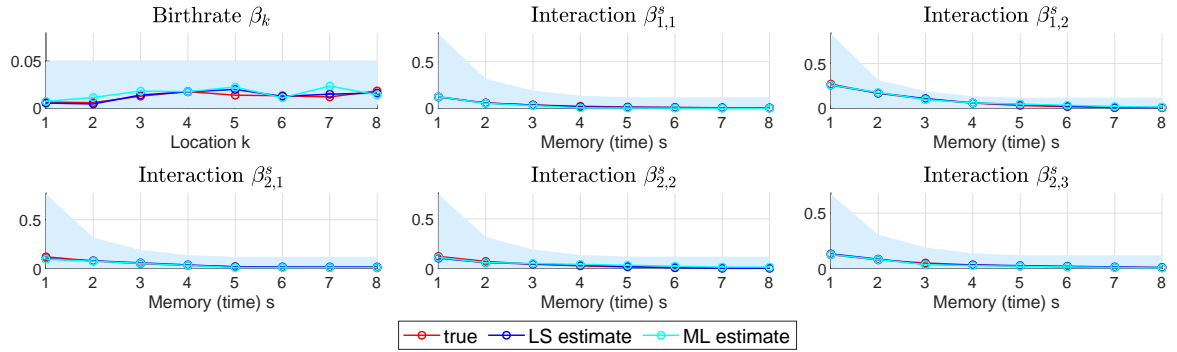


Figure 4: Single-state process estimation with 90% Confidence Intervals

## 5.2 Multi-state spatio-temporal processes

In this example, we consider a multi-state spatio-temporal Bernoulli process with the number of states being  $M = 2$ , i.e., the possible states  $p = 0, 1, 2$  (zero representing no events,  $p = 1, 2$  denotes the event of category 1 and 2, respectively). The rest of the parameters are: the memory depth  $d = 8$ , number of locations  $K = 10$ . The restrictions specifying  $\mathcal{X}$  were expressed by the constraints that

- $\beta_k(p) \geq 0$ ,  $\beta_{kl}^s(p, q) \geq 0$ ;  $\sum_{p=1}^M \beta_k(p) + \sum_{s=1}^d \sum_{\ell=1}^K \max_{0 \leq q \leq M} \sum_{p=1}^M \beta_{k\ell}^s(p, q) \leq 1, \forall k \leq K$ ;
- $\beta_{k\ell}^s(p, q) = 0$  when  $|k - \ell| > 1$ ,  $\forall p, q$  (only neighbors can affect each other);
- For every  $1 \leq k, \ell \leq K$  and  $1 \leq p \leq M, 0 \leq q \leq M$ ,  $\beta_{k\ell}^s(p, q)$  is a *non-increasing convex* function of  $s$ .

Moreover, we consider two scenarios in our experiments:

- Scenario 1: each event can only trigger the event of the same category, i.e.,  $\beta_{k\ell}^s(p, q) \equiv 0$  when  $q \neq p$ .
- Scenario 2: events in category  $q = 0, \dots, M$  only have effect on events with category  $p \leq q$ . This can happen for example, when modeling earthquakes. All possible earthquakes can be split into  $M$  groups according to their magnitudes  $u_1 < \dots < u_M$ , set  $u_0 = 0$  and treat the event “no earthquake” as “earthquake of magnitude 0.” Then each earthquake can trigger “aftershocks” with *the same or smaller* magnitudes.

We generate a synthetic data sequence of length  $N = 20,000$ , and compute the LS solution to (19), and the ML solution to (29). The recovery errors are reported in Table 2. Note that in addition to the total recovery errors, we also report two separate errors: (i) the error for the baseline intensity vector (birthrates)  $\beta_{birth} = \{\beta_k(p), k \leq K, 1 \leq p \leq M\} \in \mathbb{R}^{KM \times 1}$ ; (ii) the error for the influence (interaction between different pairs of locations)  $\beta_{inter} = \{\beta_{k,\ell}^s(p, q)\} \in \mathbb{R}^{dK^2M(M+1) \times 1}$ . Usually, the baseline intensity is much higher than the influence parameters. Therefore, the recovery error for the baseline intensities is smaller than the error for influences. Overall, the recovery error is small and indicates a successful recovery of the unknown parameters. Moreover, we compare the true influence and the recovered influence parameters in Figure 5.

Table 2: Multi-state process recovery: norms of recovery error for LS recoveries  $\hat{\beta}_{LS}$  and ML recoveries  $\hat{\beta}_{ML}$  (percents: norm of recovery error in percents of the norm of vector of true parameters).

Estimate	Scenario 1		Scenario 2	
	$\ell_1$ error	$\ell_2$ error	$\ell_1$ error	$\ell_2$ error
$\hat{\beta}_{ML}$	0.3524 (4.7%)	0.0532 (2.5%)	1.0179 (13.6%)	0.1146 (5.9%)
$\hat{\beta}_{LS}$	0.4947 (6.6%)	0.0744 (3.4%)	1.0854 (14.5%)	0.1230 (6.3%)
$\hat{\beta}_{ML,birth}$	0.0106 (2.7%)	0.0028 (3.1%)	0.0226 (5.7%)	0.0060 (6.7%)
$\hat{\beta}_{LS,birth}$	0.0160 (4.0%)	0.0044 (5.0%)	0.0237 (5.9%)	0.0066 (7.4%)
$\hat{\beta}_{ML,inter}$	0.3419 (4.8%)	0.0531 (2.5%)	0.9952 (14.0%)	0.1144 (5.9%)
$\hat{\beta}_{LS,inter}$	0.4786 (6.7%)	0.0743 (3.4%)	1.0617 (15.0%)	0.1228 (6.3%)

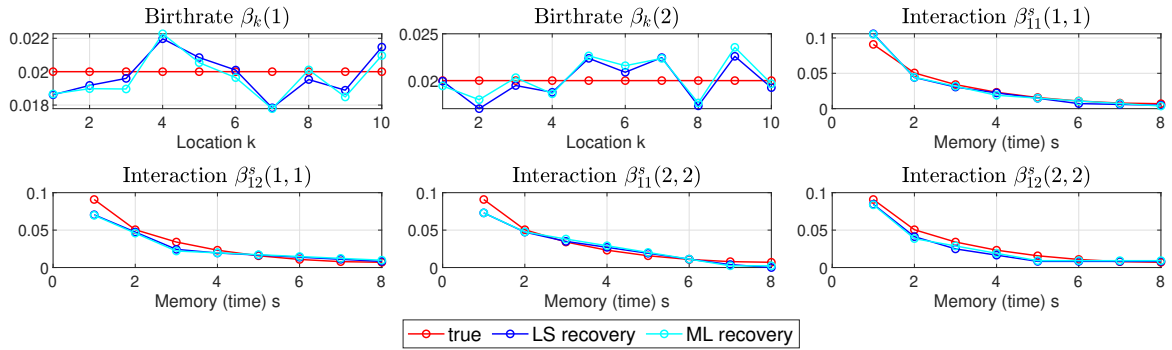


Figure 5: Multi-state process: examples of LS and ML estimates for baseline intensity  $\beta_k(p)$  and influence functions  $\beta_{k,\ell}^s(p, q)$ .

Finally, we generate one example to test the prediction power of our model. We generate a data sequence of the same length  $N = 20000$ , and compare the frequency of different categories' events that happen over the entire time horizon  $[1, N]$ . We use the past observations, using our model based on estimated parameters, to predict the probability of observing an event in the next time interval. From the result shown in Fig 6, we can see that the observed frequency and the predicted probability match quite well. This indicates the good performance of the LS and ML estimates from another perspective: the potential *prediction* power of the LS and ML estimates.

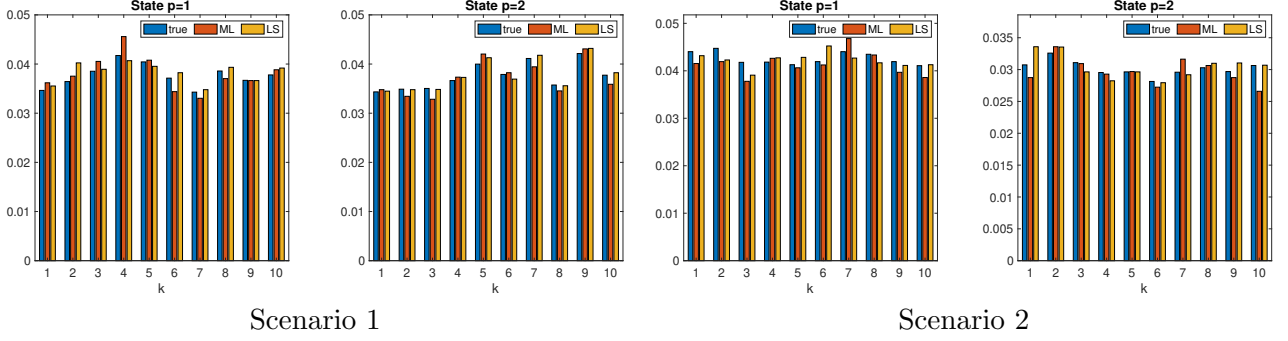


Figure 6: Multi-state process: recovered frequencies through LS and ML estimates.

### 5.3 Sparse recovery

In this subsection, we consider recovery of a sparse graph with “asynchronous” influence functions, as shown in Fig 7. Consider a directed graph with are  $K = 8$  nodes. The weights on the edges are randomly generated. The influence functions are not exponential functions but will have peaks around a delay that differs from edge-to-edge, and the delays are randomly generated as well. The purpose of this example is to demonstrate (i) the algorithm can recover the correct edges, i.e., the support of the adjacency matrix, as well as (ii) the algorithm can recover the correct shape of the influence function, without them being monotonically decaying over time.

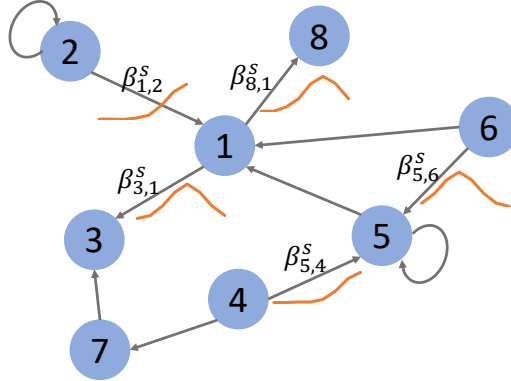


Figure 7: Sparse graph: the “asynchronous” influence function are indicated in orange.

The true parameters as generated as follows.

- The birthrate at each location is generated from a uniform distribution supported on  $[0, 0.2]$ .
- The influence functions are “asynchronous”: for each directed edge  $\ell \rightarrow k$ , the interaction  $\beta_{k,\ell}(s)$  as a function of memory  $s$  is set as  $\beta_{k,\ell}(s) = 0.05e^{-0.25(s-\tau_{k\ell})^2}$ , where the peak  $\tau_{k\ell}$  is randomly chosen from  $1, \dots, d$  for each edge  $\ell \rightarrow k$ , as illustrated in Fig 7.

In our implementation, we do not impose any sparsity assumption while solving the LS and ML problems. The goal is to explore whether the LS and ML can recover the underlying graphical structure using only the data samples. We report the recovery errors ( $\ell_1, \ell_2$ , and  $\ell_\infty$ ) in Table 3. From

the results, we can see that the overall error is reasonable and the estimate for the birthrate  $\beta_k, k \leq K$  is more accurate for the interaction parameters (transfer function).

Table 3: Sparse network recovery: errors of LS and ML estimates  $\hat{\beta}_{LS}, \hat{\beta}_{ML}$  (percents: the norm of recovery error in percents of the norm of the vector of true parameters).

Estimate	$\ell_1$ error	$\ell_2$ error	$\ell_\infty$ error
$\hat{\beta}_{ML}$	1.0272 (40.58%)	0.0858 (21.28%)	0.0184 ( 9.73%)
$\hat{\beta}_{LS}$	1.2075 (47.70%)	0.0951 (23.59%)	0.0197 (10.42%)
$\hat{\beta}_{ML,birth}$	0.0677 ( 8.80%)	0.0260 ( 8.36%)	0.0147 ( 7.77%)
$\hat{\beta}_{LS,birth}$	0.0997 (12.96%)	0.0370 (11.87%)	0.0197 (10.42%)
$\hat{\beta}_{ML,inter}$	0.9595 (54.46%)	0.0817 (31.97%)	0.0184 (36.79%)
$\hat{\beta}_{LS,inter}$	1.1078 (62.88%)	0.0876 (34.26%)	0.0185 (36.91%)

Moreover, we compare the recovered interaction parameters with the true parameter in Figure 8. It can be seen that: (i) for pairs  $(k, l)$  such that there is a directed edge from node  $l$  to node  $k$ , the recovered parameters  $\beta_{k,l}(s), s \leq d$  indeed matches the true parameter closely; (ii) for pairs  $(k, l)$  that does not have an edge between them, the recovered parameters are almost zero. Therefore, both the LS and ML estimates can recover the underlying graph structure accurately if we set the threshold properly to filter out those edges with negligible estimators.

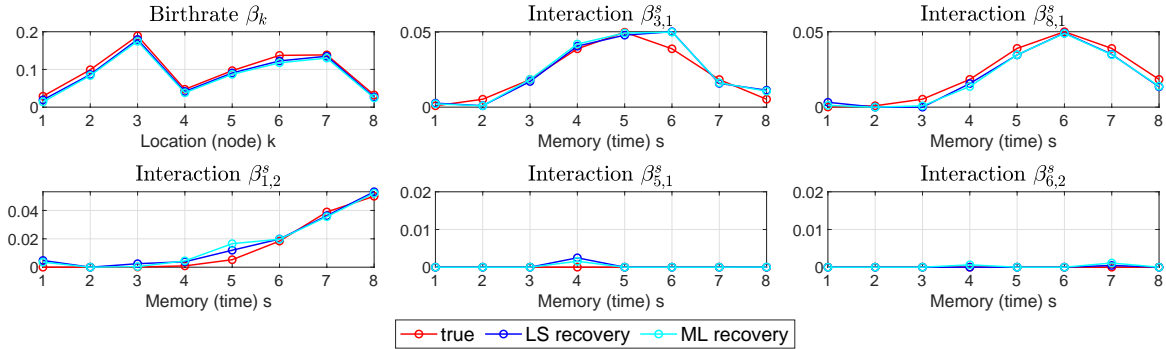


Figure 8: Sparse network recovery: examples of LS and ML estimates for baseline intensity and influence functions; the upper left corresponds to the baseline intensity, while others correspond to the influences. The lower middle and right correspond to edges that does *not* exist in Graph 7.

In summary, even when we do not have prior information about the spare structure of the underlying network, the LS and ML estimates are able to recover the underlying network flow based on data itself. This is of great importance and can be applied to problems like casual inference [16].

## 6 Real data study

### 6.1 Crime events in Atlanta

We apply the proposed method to a real crime dataset in Atlanta city. This dataset contains the “burglary” and “robbery” crime events reported to the Atlanta Police Department from January 1, 2015

to September 19, 2017, including 47,245 “burglary” events and 3,739 “robbery” events. Therefore, this dataset can be viewed as a multi-state spatial Bernoulli process with state number  $\pi = 3$ , and all possible states include: no event ( $p = 0$ ), burglary ( $p = 1$ ) and robbery ( $p = 2$ ).



Figure 9: Raw data map: burglary and robbery incidents in Atlanta. Left: the full map; Right: zoom-in around downtown Atlanta.

Due to the massive amount of crime events and their widely spread locations, we perform the pre-processing to extract crime events around the Atlanta downtown area, as shown in Fig9. After truncation, we have 427 “burglary” events and 38 “robbery” events. The continuous two-year time period is split into discrete time intervals with equal duration: each interval stands for four hours. The zoom-in region is divided uniformly into 16 sub-regions. After truncation, the event times at each sub-region are shown in Fig 10, from which we can see that the Robbery event is much less than the Burglary event.

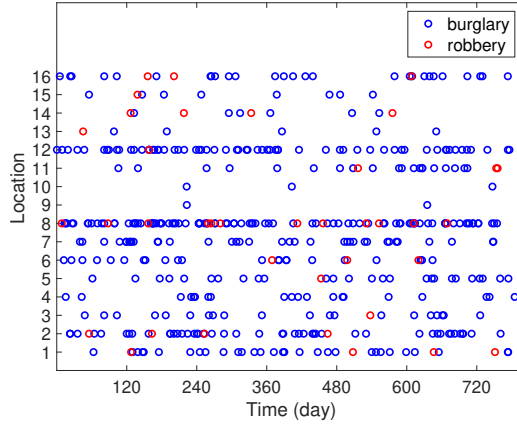


Figure 10: Raw data: times of burglary and robbery events in a 2-year time period.

We apply the Least Square methods to estimate the underlying parameters  $\{\beta_k(p), \beta_{k,l}^s(p, q)\}$ . We consider two situations while solving the Least Square problem

- Impose the non-increasing and convexity constraint for the influence parameters (or the transfer function);

- Do not impose the non-increasing and convexity constraint for the influence parameters (or the transfer function).

The first situation with non-increasing and convexity constraints is widely seen in the Hawkes model and is assumed to match various real data problems. Here we also consider the second case without those constraints because they provide more general solutions to the spatio-temporal Bernoulli process.

We illustrate the learned parameters in Fig 16. The dot in each region denotes the learned birthrate for Burglary/Robbery events, i.e.,  $\beta_k(p)$ ,  $k = 1, \dots, K$ ; the width of the arrow denotes the size of the influence between nodes, i.e.,  $\beta_{k,l}^s(p, q)$ . Moreover, we also simulate a new two-year sequence based on the LS estimate and then compare the frequency of Burglary and Robbery events. The results are shown in Table 4. Note that the frequency of Robbery events matches better with real data, and the results obtained without imposing the non-increasing and convexity constraint are better in several locations. It is worth emphasizing that here frequency recovery is not our ultimate goal for real crime dataset; the results are shown in Table 4 only serves as a simple illustration of how the frequency that is randomly generated from the estimated parameters coincides with the frequency for the true dataset. The accuracy here may shed light on the prediction performance using estimated parameters.

Table 4: Crime recovery: the frequency of Burglary and Robbery events at each location.

Locations	Burglary			Robbery		
	True	With constr	Without constr	True	With constr	Without constr
1	0.0064	<b>0.0081</b>	0.0100	0.0008	<b>0.0008</b>	0.0013
2	0.0098	0.0110	<b>0.0108</b>	0.0008	0.0021	<b>0.0008</b>
3	0.0042	0.0068	<b>0.0059</b>	0.0002	0.0015	<b>0.0008</b>
4	0.0042	<b>0.0062</b>	0.0070	0.0000	0.0004	0.0004
5	0.0055	<b>0.0085</b>	0.0096	0.0002	0.0004	<b>0.0002</b>
6	0.0047	<b>0.0051</b>	0.0079	0.0006	0.0017	<b>0.0008</b>
7	0.0076	0.0123	<b>0.0072</b>	0.0000	0.0008	<b>0.0004</b>
8	0.0187	0.0227	<b>0.0200</b>	0.0025	<b>0.0042</b>	0.0064
9	0.0004	0.0013	<b>0.0011</b>	0.0000	0.0004	<b>0.0002</b>
10	0.0006	0.0021	0.0021	0.0000	0.0000	0.0000
11	0.0042	<b>0.0059</b>	0.0062	0.0006	0.0006	0.0006
12	0.0127	0.0149	<b>0.0146</b>	0.0000	0.0019	<b>0.0015</b>
13	0.0011	<b>0.0015</b>	0.0019	0.0002	0.0006	<b>0.0004</b>
14	0.0013	0.0032	<b>0.0017</b>	0.0008	<b>0.0011</b>	0.0019
15	0.0017	0.0028	<b>0.0021</b>	0.0002	<b>0.0002</b>	0.0006
16	0.0057	<b>0.0059</b>	0.0070	0.0006	0.0017	<b>0.0015</b>

## 6.2 Novel coronavirus spread in China

Recently, the novel coronavirus outbreak caused by the 2019 novel coronavirus disease (COVID-19) has been studied intensively. We aims to study the outbreak from a statistical perspective and apply the Bernoulli process to model the nationwide spread pattern of the coronavirus disease in China. To start with, we first model the spread as a single-state Bernoulli process; the extension to multi-state Bernoulli process will be discussed later.



Table 5: Crime recovery: the concentration recovery at location 1.

Window Length	True	With constr	Without constr	Guess
2	0.0000	0.0000	0.0000	0.0001
3	0.0000	0.0004	0.0013	0.0002
4	0.0002	0.0011	0.0017	0.0003
5	0.0004	0.0021	0.0021	0.0005
6	0.0006	0.0034	0.0030	0.0008
7	0.0009	0.0047	0.0038	0.0011
8	0.0011	0.0062	0.0049	0.0014
9	0.0013	0.0072	0.0062	0.0018
10	0.0015	0.0085	0.0072	0.0023

Table 6: Crime recovery: the concentration recovery at location 6.

Window Length	True	With constr	Without constr	Guess
2	0.0000	0.0000	0.0000	0.0000
3	0.0000	0.0008	0.0004	0.0001
4	0.0000	0.0011	0.0011	0.0002
5	0.0002	0.0011	0.0011	0.0003
6	0.0004	0.0011	0.0011	0.0004
7	0.0006	0.0015	0.0011	0.0006
8	0.0011	0.0017	0.0011	0.0008
9	0.0015	0.0019	0.0013	0.0010
10	0.0019	0.0023	0.0017	0.0012

The dataset we use is a one-month dataset from 01/19/2020 to 02/16/2020, which is the major time period for the coronavirus outbreak in China. The time interval is approximately 30 minutes, and the data contains the number of confirmed patients for every 30 minutes at 34 *Provincial Administrative Regions*. In the analysis, we exclude the Hubei province due to its dominance in the number of confirmed patients and its strong governmental intervention.

We first define what is an “event” in the single state Bernoulli model. We have  $K = 33$  locations, and the time interval  $\Delta_t = 0.5$  hour, denote the *increase* of the confirmed patients during time  $[(t-1)\Delta_t, t\Delta_t)$  as  $N_k^t$ , then we define

$$\omega_{tk} = \begin{cases} 1 & N_k^t \geq 1 \\ 0 & N_k^t = 0 \end{cases}$$

In other words,  $\omega_{tk}$  is an indicator of whether the number of confirmed patients have increased in the  $t$ -time interval. The above model can be extended to multi-state by considering the magnitude of the increase. We plot the overall frequency of event happening at 33 different regions in Fig 11.

We set the memory depth to be 6 hours and solve the Least Square estimation for the underlying parameters, including the birthrates and the interaction effects. Note that we impose the *sparsity* constraint to ensure that each region will only affect its neighboring regions (such neighborhood is measured by a Euclidean ball in the map); while we do *not* impose any convexity or non-increasing

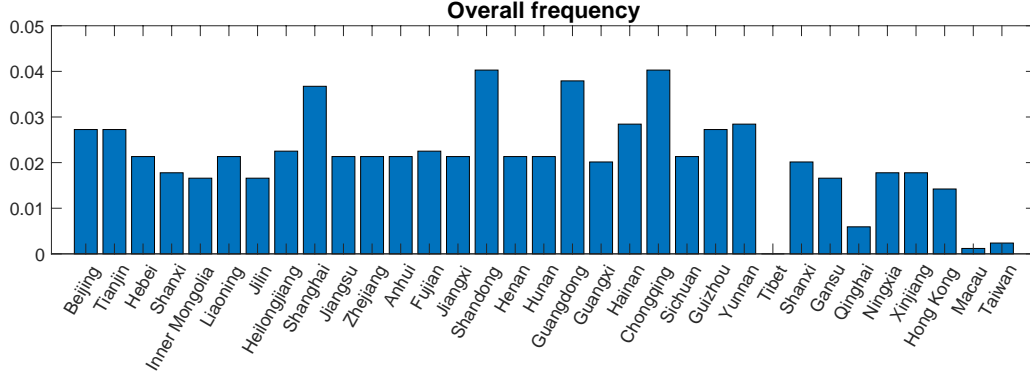


Figure 11: COVID-19 raw data: the overall frequency over one month 01/19/2020-02/16/2020.

constraint while solving the Least Square solution. The results are illustrated in Fig 12. Moreover, we plot several representative interaction functions in Fig 14.

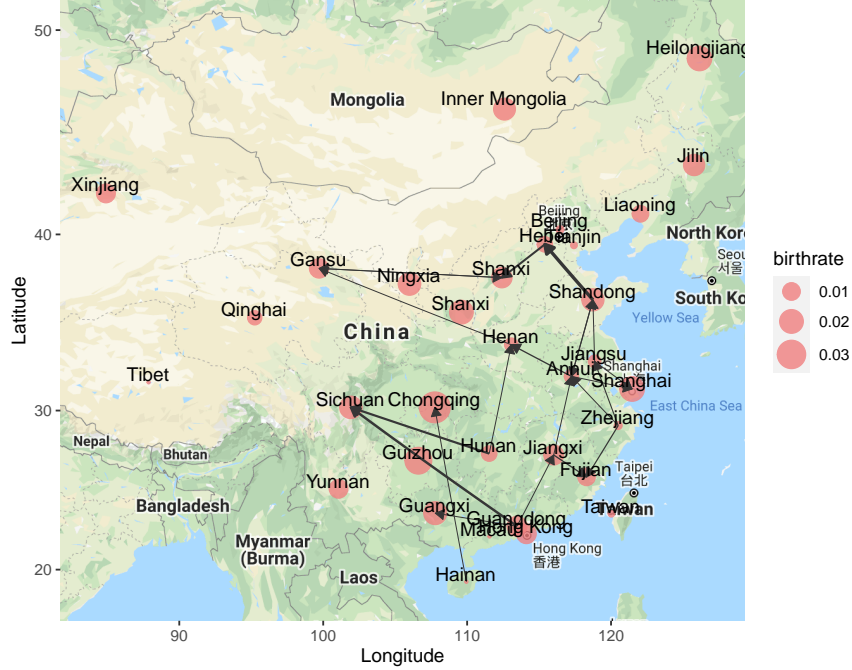


Figure 12: COVID-19 data modeling: graphical illustration of the Least Square estimate for the single state Bernoulli model for COVID-19 data in China.

Note that since we do not assume that the parameters decays monotonically from the moment of the event occurs, our estimated influence function can capture the effect of “delayed” influence. For example, from the Least Square estimates, we estimated that the influence of Tianjin’s cases to Beijing has a delay of 3.5 hours (in the sense that the peak of the influence is achieved at 3.5 hours). Further analysis will be performed to study the prediction performance of the single state model and the extension to multi state model.

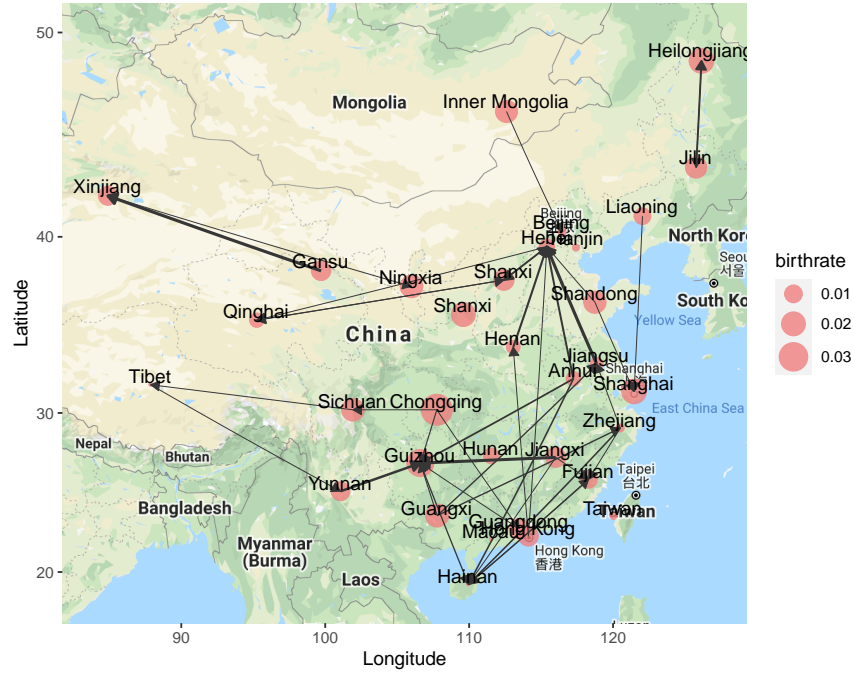


Figure 13: COVID-19 data modeling: graphical illustration of the Least Square estimate for the single state Bernoulli model using a larger network.

## 7 Conclusion

In this work, we have considered a discrete-time Bernoulli process model, with the goal to capture the spatial-temporal dependence of events. Bernoulli process, whose observations are binary (to indicate whether or not an event has happened) is a natural simplification of the continuous-time Hawkes process, in the discrete-time and discrete space setting. Similar to other self- and mutual point processes models, we model dependence and triggering effect through linear linkage and general linkage functions. A notable feature of our model is that we allow the influence function to be completely general, for example (1) the influence does not have to be monotonically decaying, which is a common assumption used in existing work; (2) the influence function can have delays, which is an aspect largely ignored in existing work since most work assumes that the influence kernel function is a monotonic decaying function that starts immediately from the event time. This generality comes because we can incorporate almost arbitrary assumptions (or non-assumption) through the constraints. We cast the influence function recovery problem using two approaches: (1) the least-square (LS) estimate, and (2) the maximum likelihood (ML) estimate. We take a variational inequality formulation to address the resulted optimization problem, which enables us to obtain interpretable performance bounds and confidence intervals for the estimates, and computationally efficient algorithms. We demonstrate the good performance of our LS and ML estimators on simulated experiments and using real-world data, in estimating the influence functions on crime data and the spread of recent novel coronavirus. Future work includes extensions of our approach to Poisson observations, i.e., the observations at each time, and each location is a count.

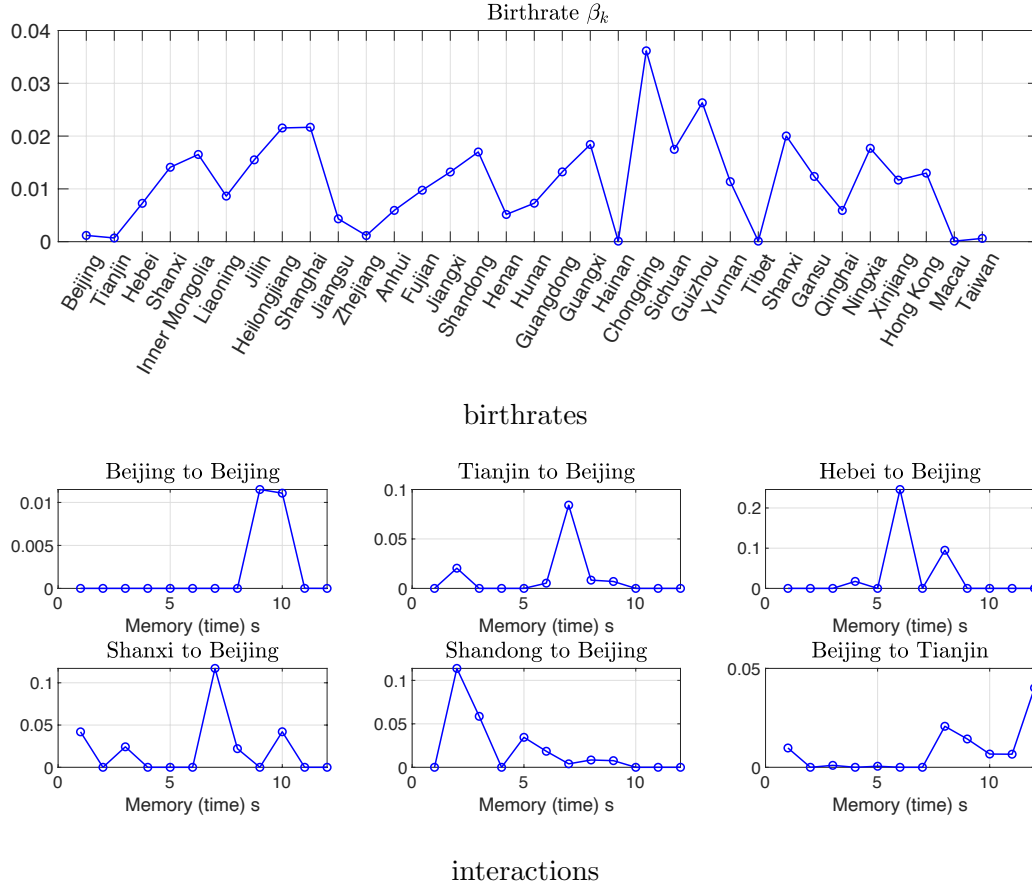


Figure 14: COVID-19 data modeling: representative Least Square estimates for the birthrates and interaction between different regions.

## Acknowledgement

The authors would like to thank Dr. Shihao Yang for providing the one-month novel coronavirus dataset used in Section 6.2. This work is partially supported by CCF-1650913, DMS-1830210, and DMS-1938106.

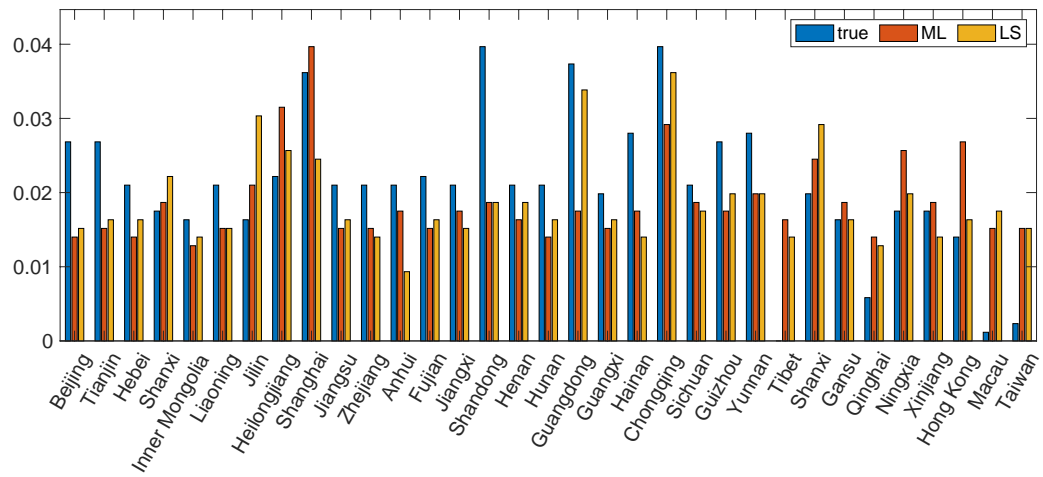
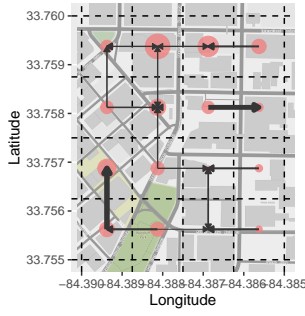
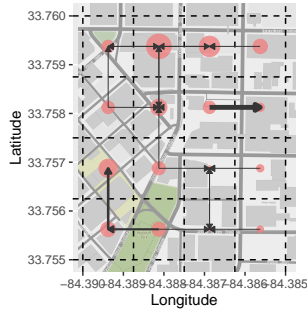


Figure 15: COVID-19 data modeling: recovered frequencies of event happening at 33 different regions.

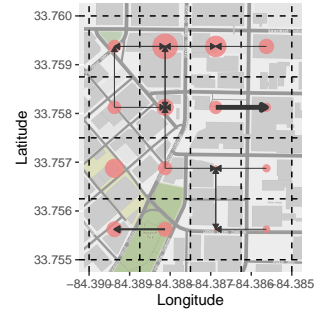
### Burglary to Burglary



$s = 1$

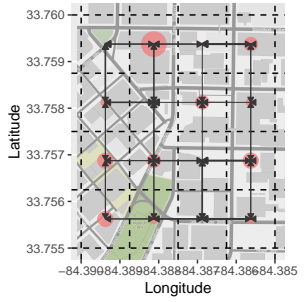


$s = 3$

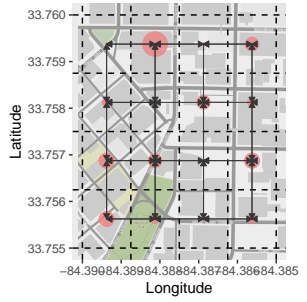


$s = 6$

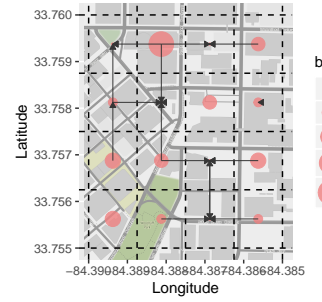
### Robbery to Robbery



$s = 1$

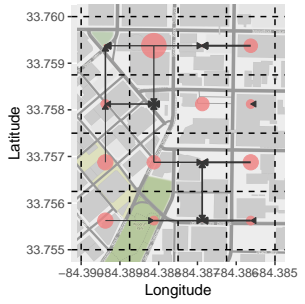


$s = 3$

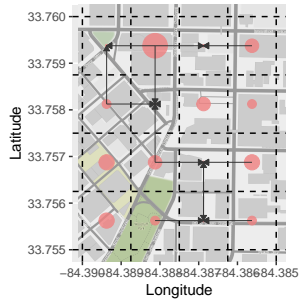


$s = 6$

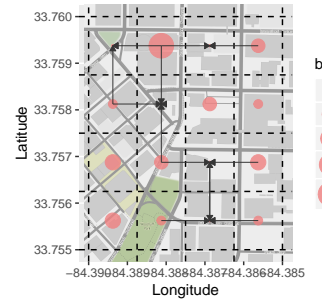
### Burglary to Robbery



$s = 1$

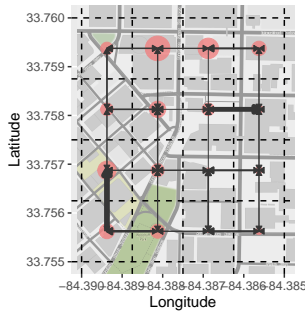


$s = 3$

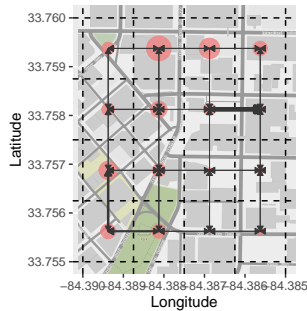


$s = 6$

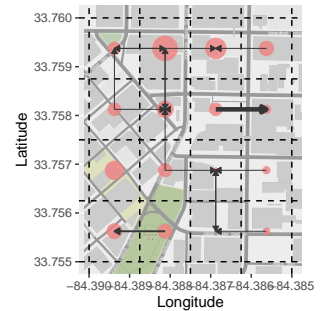
### Robbery to Burglary



$s = 1$



$s = 3$



$s = 6$

Figure 16: Crime recovery: the illustration of the LS estimated influence between events.

## References

- [1] Shizhe Chen, Ali Shojaie, Eric Shea-Brown, and Daniela Witten. The multivariate hawkes process in high dimensions: Beyond mutual excitation. *arXiv preprint arXiv:1707.04928*, 2017.
- [2] Şeyda Ertekin, Cynthia Rudin, Tyler H McCormick, et al. Reactive point processes: A new approach to predicting power failures in underground electrical systems. *The Annals of Applied Statistics*, 9(1):122–144, 2015.
- [3] Eric Warren Fox, Frederic Paik Schoenberg, Joshua Seth Gordon, et al. Spatially inhomogeneous background rate estimators and uncertainty quantification for nonparametric hawkes point process models of earthquake occurrences. *The Annals of Applied Statistics*, 10(3):1725–1756, 2016.
- [4] Manuel Gomez-Rodriguez, Jure Leskovec, and Bernhard Schölkopf. Modeling information propagation with survival theory. In *International Conference on Machine Learning*, pages 666–674, 2013.
- [5] Alan G Hawkes. Point spectra of some mutually exciting point processes. *Journal of the Royal Statistical Society: Series B (Methodological)*, 33(3):438–443, 1971.
- [6] Alan G Hawkes. Spectra of some self-exciting and mutually exciting point processes. *Biometrika*, 58(1):83–90, 1971.
- [7] Alan G Hawkes and David Oakes. A cluster process representation of a self-exciting process. *Journal of Applied Probability*, 11(3):493–503, 1974.
- [8] Eric L Lai, Daniel Moyer, Baichuan Yuan, Eric Fox, Blake Hunter, Andrea L Bertozzi, and P Jeffrey Brantingham. Topic time series analysis of microblogs. *IMA Journal of Applied Mathematics*, 81(3):409–431, 2016.
- [9] George Mohler et al. Modeling and estimation of multi-source clustering in crime and security data. *The Annals of Applied Statistics*, 7(3):1525–1539, 2013.
- [10] George O Mohler, Martin B Short, P Jeffrey Brantingham, Frederic Paik Schoenberg, and George E Tita. Self-exciting point process modeling of crime. *Journal of the American Statistical Association*, 106(493):100–108, 2011.
- [11] Jesper Moller and Rasmus Plenge Waagepetersen. *Statistical inference and simulation for spatial point processes*. CRC Press, 2003.
- [12] Yu Nesterov. Semidefinite relaxation and nonconvex quadratic optimization. *Optimization methods and software*, 9(1-3):141–160, 1998.
- [13] James Pitkin, Ioanna Manolopoulou, and Gordon Ross. Bayesian hierarchical modelling of sparse count processes in retail analytics. *arXiv preprint arXiv:1805.05657*, 2018.
- [14] André Python, Janine Illian, Charlotte Jones-Todd, and Marta Blangiardo. A bayesian approach to modelling fine-scale spatial dynamics of non-state terrorism: world study, 2002-2013. *arXiv preprint arXiv:1610.01215*, 2016.

- [15] Alex Reinhart. A review of self-exciting spatio-temporal point processes and their applications. *arXiv preprint arXiv:1708.02647*, 2017.
- [16] Alex Tank, Emily B Fox, and Ali Shojaie. Granger causality networks for categorical time series. *arXiv preprint arXiv:1706.02781*, 2017.
- [17] Baichuan Yuan, Hao Li, Andrea L Bertozzi, P Jeffrey Brantingham, and Mason A Porter. Multivariate spatiotemporal hawkes processes and network reconstruction. *SIAM Journal on Mathematics of Data Science*, 1(2):356–382, 2019.